# Revision 1

# Thallium geochemistry in the metamorphic Lengenbach sulfide deposit, Switzerland: thallium-isotope fractionation in a sulfide melt

Kai Hettmann*[a], Katharina Kreissig[b], Mark Rehkämper[b,], Thomas Wenzel[a], Regina Mertz-Kraus[c] and Gregor Markl[a]

*corresponding author:
email: kai.hettmann@uni-tuebingen.de
tel.: +49-(0)7071-29-73165
fax: +49-(0)7071-29-3060
Author's addresses:
[a]Fachbereich Geowissenschaften, Eberhard Karls Universität Tübingen, Wilhelmstraße 56, 72074 Tübingen, Germany
[b]Department of Earth Science and Engineering, Imperial College London, United Kingdom
[c]Institut für Geowissenschaften, Johannes Gutenberg-Universität Mainz, Germany

## Abstract

The Lengenbach (Switzerland) Pb-As-Tl-Zn deposit was formed from a sulfide melt at about 500 °C during Alpine metamorphism, but details on its formation and especially the source of the metals are still under debate. In this study we present two sample sets to address these questions:

1. MC-ICP-MS analyses of thallium isotopes in sulfides, sulfosalts and melt inclusions from the Alpine metamorphic Lengenbach deposit in the Binn valley of Switzerland, the non-metamorphic Wiesloch Mississippi Valley-type deposit in Southern Germany, and the Cu- and As-rich mineralization at Pizzo Cervandone about 2 km SW of the Lengenbach deposit, which has been discussed as potential source of the Lengenbach metals.
2. LA-ICP-MS analyses of micas from the Lengenbach deposit and surrounding country rocks between the deposit and the Pizzo Cervandone to trace potential metal-bearing fluid pathways.

We found that Tl isotope compositions expressed as $\varepsilon^{205}$Tl values in all investigated samples range from -4.1 ± 0.5 to +1.9 ± 0.5. The whole variation can be seen in the Lengenbach deposit alone, which hence records considerable fractionation even during high-temperature processes involving a sulfide melt. This large range of $\varepsilon^{205}$Tl is thought to be caused by nuclear volume-dependent fractionation. Interestingly, the common fahlores at Lengenbach behave differently from all other investigated sulfosalts: based on their heavy isotopic composition together with a low As/S-ratio, they do not seem to be crystallized from the sulfide melt, but are interpreted to have formed from hydrothermal fluids enriched in the heavy Tl isotopes.

Although As mobilization in the gneisses and dolomites surrounding the Lengenbach deposit is evident based on secondary arsenites, no traces of such a country rock fluid could be found in fissure micas at Lengenbach. Hence, considerations involving K/Rb, Rb/Tl, As/S and Pb/Tl ratios in the sulfides and micas imply that the element enrichment in the Lengenbach deposit is either pre-Alpine or related to peak metamorphism, but occurred definitely before mica growth at Lengenbach.

## Introduction

The Lengenbach Pb-As-Tl-Zn deposit (Binn Valley/Switzerland) is well known for the occurrence of rare Tl-bearing sulfosalts and sulphides (Giusca 1930; Graeser 1965, 1975; Hofmann and Knill 1996; Graeser et al. 2008). It is the type locality of 31 mineral species, 16 of which have only been described from here (Hofmann et al. 1993; Graeser et al. 2008). This mineralogical diversity has been investigated in numerous publications since its discovery in the 19th century (Giusca 1930; Graeser 1965, 1975; Graeser et al. 2008).

The Lengenbach deposit formed under participation of a sulfide melt generated during regional metamorphism (Hofmann 1994). This process has been involved even in the generation of some world class deposits, such as Broken Hill in Australia (Sparks and Mavrogenes 2005; Tomkins et al. 2007). A sulfide melt is produced if metamorphic temperatures are high enough to melt a precursor sulfide mineralization. The required temperature depends on the primary mineral composition, the mineral assemblages and $f_{O2}$. In the course of fractional crystallization of the sulfide melt (Tomkins et al. 2007) As and Tl behave as incompatible elements. They are strongly enriched in the remaining melt fraction from which minerals such as jordanite and dufrenoysite crystallize.

Although the Lengenbach deposit was the subject of many scientific investigations, details of its formation and especially the source of the metals are still under debate: both the formation by melting of a hypothetical precursor mineralization (under nearly closed system conditions) and an external elemental input were discussed in the literature (e.g. Graeser and Roggiani 1976; Hofmann and Knill 1996).

In this study we determined the chemical and Tl isotopic composition of various Tl-bearing sulfosalts, sulfides and micas from the Lengenbach quarry in the Lengenbach deposit. The unusual diversity of Tl-bearing minerals at the Lengenbach quarry makes it an ideal target for the exploration of the potential use of the new analytical method of Tl isotope composition on ore

deposits (Rehkämper and Halliday 1998). For comparison, we also analyzed the Cu-As mineralization in pre-Alpine gneisses of the Pizzo Cervandone south of the Lengenbach quarry and a Mississippi Valley-type deposit at Wiesloch, South Germany. Alpine mobilization of the Pizzo Cervandone mineralization has been invoked in models to explain the chemical inventory of the Lengenbach deposit (Graeser 1965; Graeser and Roggiani 1976) while the Wiesloch Mississippi Valley-type deposit has been considered as a non-metamorphic analogue for the precursor mineralization of Lengenbach (Hofmann and Knill 1996; Pfaff et al., 2010). The main purpose of this study was to obtain new insight into the formation of the Lengenbach deposit and the behavior of Tl isotopes during sulfide melt formation and evolution. Mica fractions from various fissures in different host rocks in the Binn valley were additionally investigated to reconstruct potential pathways of Tl-bearing fluids or interaction with a sulfide melt.

## Geology

The Lengenbach deposit is located in southern Switzerland in the Penninic units of the Alpine realm (Hofmann and Knill 1996). It occurs in metamorphosed Triassic dolomites in the Binn Valley (Fig. 1). Peak metamorphic conditions were determined in the Steinental close to the Binn Valley as upper greenschist to lower amphibolite facies (around 500 to 520 ºC and 6.5 to 7.5 kbar) at 28 Ma ago (Frey et al. 1974; Vance and O'Nions 1992; Hofmann and Knill 1996).

Mineralized Triassic dolomites are located between a basement of granitic gneisses of the Monte Leone nappe and the overlying Bündnerschiefer (Fig. 1). The pre-Alpine basement is built up by Permian metasediments and meta-volcanics, and pre-Permian orthogneisses. The Bündnerschiefer consist of metamorphosed carbonate-rich sandstones and marls deposited during the extension of the Penninic basin and intercalated metamorphosed basalts. The dolomites hosting the mineralization are interpreted to have formed as platform dolomites during the beginning of the Penninic extension (Hofmann and Knill 1996; Galster in press).

Triassic dolomites occurring in the Binn Valley area can be subdivided into two strata, the Lengenbacher stratum and the Feldbacher stratum (Fig. 1), at which the position of the locality Balmen is unclear, but most probably a part of the Lengenbacher stratum. The dolomites hosting the Lengenbach deposit are located in the Lengenbacher stratum and have a thickness of about 240 m. The mineralized zone is located close to the crystalline basement (Graeser 1965, 1975; Hofmann and Knill 1996). The major part of the mineralization consists of stratabound layers containing up to 80 vol% pyrite and smaller layers of sphalerite and galenite (Hofmann and Knill 1996), all with various kinds of rare sulfosalts. These layers can be subdivided into a reduced zone, an As(III)-rich zone and an intermediate redox zone (in stratigraphic order). The reduced zone is characterized by the occurrence of pyrite, pyrrhotite, arsenopyrite, sphalerite, magnetite, biotite and uraninite. The As(III)-rich zone is composed of pyrite, barite, sphalerite, baumhauerite, sartorite, orpiment, realgar and other As-rich sulfosalts (see Tab. 1). In this zone, Pb-Tl-rich sulfide melt inclusions in quartz have been identified and discordant veinlets containing baumhauerite, sartorite, realgar and dufrenoysite are found (Hofmann and Knill 1996). The intermediate redox zone consists of pyrite, barite, galena, sphalerite, jordanite and other As-poor sulfosalts. In addition to these stratigraphically confined zones, mineral druses and open fissures containing a large number of euhedral sulfosalts (>50 different species) and micas have been identified (Hofmann et al. 1993; Graeser et al., 2008).

The formation of the Lengenbach deposit has been interpreted to be the result of a sulfide melt generated at Alpine peak metamorphic conditions (Hofmann 1994). This sulfide melt underwent fractional crystallization of sulfosalts such as jordanite, which resulted in the enrichment of As and Tl, and the depletion of Pb in the remaining melt fractions. This is shown by compositional trends of melt inclusions, namely the enrichment of As and the depletion of Pb (Hofmann 1994), and the succession of more As-rich minerals observed in the Lengenbach deposit. Early phases include e.g. rathite and jordanite, late phases e.g. baumhauerite and sartorite (Giusca 1930). In addition, the

125 presence of a hydrothermal aqueous fluid during and after the crystallization of the sulfide melt was
126 proposed to be responsible for the formation of mica and quartz in open fissures (Hofmann et al.
127 1993).
128 In addition to the Lengenbach deposit, samples from mineralized orthogneisses at Pizzo
129 Cervandone in the Binn Valley area (Fig. 1) have been investigated in this study as they are thought
130 to represent a possible metal source for Lengenbach (Graeser 1975). At Pizzo Cervandone,
131 basement orthogneisses host a pre-Alpine Cu-As mineralization consisting of sulfide minerals
132 (Graeser and Roggiani 1976; Guastoni et al. 2006) and Alpine veins with unusual arsenite minerals
133 (e.g. cafarsite, asbecasite, cervandonite). The major sulfide mineral is fahlore (tennantite) that is
134 associated with quartz and mica in cm-thick veins. Fahlore is partly altered to copper carbonates,
135 and occurs with minor pyrite, chalcopyrite and molybdenite. The Alpine fissures contain abundant
136 arsenates, arsenites, phosphates and fluorite (Graeser and Roggiani 1976). The most remarkable
137 among these are cervandonite-(Ce), gasparite-(Ce), paraniite-(Y), cafarsite, asbecasite and fetiasite,
138 which have their type locality in the Binn area (Graeser and Roggiani 1976; Armbruster et al. 1988;
139 Graeser et al. 1994; Demartin et al. 1994. The occurrence of arsenates and arsenites has been
140 interpreted to be a result of the remobilization of the orthogneiss-hosted tennantite (Guastoni et al.
141 2006).
142 Samples from the Mississippi Valley-type deposit at Wiesloch were also included in our
143 investigation since it can be regarded as a non-metamorphic equivalent of Lengenbach. The deposit
144 at Wiesloch formed during the extension of the Upper-Rhine graben in Muschelkalk dolomites at
145 temperatures of about 150°C (Pfaff et al. 2010). The mineralization consists of calcite, dolomite,
146 barite, sphalerite, galena, pyrite and subordinate sulfosalts like the Tl-bearing hutchinsonite.
147
148
149 **Samples**

We analyzed two sample sets in this study which are interconnected through the Lengenbach deposit: the first sample set comprises sulfides and melt inclusions from Lengenbach, the Pizzo Cervandone mineralizations and the Wiesloch Mississippi Valley-type deposit in Southern Germany. These samples were analyzed for their Tl isotope composition. All samples from Lengenbach are hosted by dolomite. Jordanite occurs as massive aggregates in dolomite (intermediate redox zone, see above), whereas sartorite, edenharterite and fahlore are isolated euhedral crystals grown in vugs of the As(III)-rich zone. Orpiment occurs as thin fissure covers (see Graeser 1965, 1975; Hofmann and Knill 1996 for more details). Sulfide melt inclusions investigated and described by Hofmann (1994) were investigated in our study.

Samples from the deposit at the Pizzo Cervandone include fahlores (see Tab. 2) found in granitic gneisses and the arsenite mineral asbecasite grown as euhedral free crystals in fissures. The mode of occurrence of these minerals has been described by Graeser and Roggiani (1976).

Samples from Wiesloch include banded sphalerite (schalenblende) and massive galenite that have been investigated and described by Pfaff et al. (2010).

The second sample set involves various types of micas from fissures in different host rocks sampled all over the Binn valley including the Lengenbach deposit (for details on every sample see Tab. 3). These micas were analyzed for their Tl concentrations. Most mica samples are muscovite (12), but one sample of biotite was also analyzed. The samples are from fissures hosted by granitic gneisses or by dolomite of the Lengenbacher and Feldbacher strata. The dolomite at Balmen could not clearly be attributed to one of these strata and will therefore be discussed separately. The micas used in this study occur together with a wide range of other minerals as follows (sample number of the mica fraction in parentheses):

Sulfides including pyrrhotite (Bin30) and galenite (Bin23); sulfosalts including jordanite (Bin19), arsenopyrite (Bin26) and tennantite (Bin20, Bin23); carbonates including dolomite (Bin21), calcite (Bin28), azurite, malachite (both Bin20) and synchisite (Bin25) and silicates including quartz

(Bin22), chrysocolla (Bin23), talc (Bin21), stilbite (Bin28), turmaline and allanite (both in Bin25). In addition, oxides such as magnetite (Bin24, B5108), hematite and rutile (B5108), the arsenites graeserite and asbecasite and native gold (all three in Bin26) are found together with some of the fissure micas.

## Analytical methods

### *Electron microprobe analysis*

The major element compositions of the sulfosalts (As, S, Tl, Mn, Sb, Bi, Cu, Ag, Zn, Pb and Fe) and fissure micas (Na, K, Ca, Mg, Fe, Mn, Al, Ti, Cr, Si, F and Cl ) were determined quantitatively using a JEOL JXA-8900RL Superprobe at the Fachbereich Geowissenschaften, Universität Tübingen. For the sulfosalts we applied the same analytical conditions as Staude et al. (2010), the micas were analyzed at 15 KV and 20 nA.

### *Tl isotope composition of sulfides, sulfosalts and melt inclusions*

For Tl isotope measurements, hand-picked samples were dissolved in aqua regia and subsequently evaporated and redissolved in conc. HCl several times. Tl was then separated from the sample matrix following an isotope analysis only version of the two-stage anion-exchange chromatography described by Baker et al. (2009). All isotope measurements were performed using the Nu Plasma HR multi-collector inductively coupled plasma mass spectrometry (MC-ICP-MS) (Nu Instruments) at Imperial College London. A 5 % aliquot was used to determine the Tl concentration of each sample and to determine concentration levels as well as to ensure separation from Pb had been achieved. Subsequently, individual matching reference solutions (with the same Pb and Tl concentrations) were prepared using the NIST SRM 981 Pb and NIST SRM 997 Tl reference solutions. The measured $^{205}Tl/^{203}Tl$ ratio of each sample was mass-bias corrected relative to the $^{208}Pb/^{206}Pb$ ratio of the Pb reference material NIST SRM 981 (Ketterer et al. 1991), which had been

mixed to each sample as well as to the matching reference solutions. Based on data obtained for multiple analyses of many samples and the matching standards, uncertainties (2SD) are typically ±0.5 $\varepsilon^{205}$Tl and better than ±0.7 $\varepsilon^{205}$Tl throughout (Table 4). Results of reference material analyses, which show excellent agreement with literature values, can also be found in Table 4.

*Trace element composition of fissure micas*

Trace element contents were determined on polished mineral separates using the laser ablation ICP-MS (LA-ICP-MS) facility at the Institut für Geowissenschaften, Universität Mainz, equipped with an ESI NWR 193 excimer laser system coupled to an Agilent 7500ce quadrupole ICP-MS. On each grain up to 4 spots were analyzed, 34 isotopes (including $^{75}$As, $^{85}$Rb, $^{203}$Tl and $^{205}$Tl) were monitored although this study is focused on the concentration of Tl and the large ion lithophile elements (LILE), specifically Rb. We used a dwell time of 10 ms for each mass (except 50 ms for $^{203}$Tl and $^{205}$Tl). A single spot analysis consists of 20 s background, 40 s ablation, and 20 s wash out. A laser beam diameter of 50 µm was used and the pulse repetition rate was set to 10 Hz. Energy density during ablation was around 5 J cm$^{-2}$. Before and after about 30 spots on the samples, reference materials were analyzed, including the synthetic NIST SRM 610 as calibration material and NIST SRM 614, USGS BCR-2G and GSD-1G as quality control materials (QCM). For data reduction we used the software GLITTER 4.0 (www.glitter-gemoc.com) applying the preferred values for NIST SRM 610 reported in the GeoReM database (http://georem.mpch-mainz.gwdg.de/, Application Version 15, March 2013) (Jochum, 2005, 2011) as the "true" concentrations. All measured isotope intensities were normalized to $^{29}$Si. $SiO_2$ contents applied for the samples were previously determined by EMPA; for the QCM we used the preferred values of the GeoReM database. For BCR-2G, the current version of the GeoReM database reports no preferred value for Tl. Therefore we applied as the "true" Tl concentration the value determined recently by Nielsen and Lee (2013). For the QCM, relative standard deviation (RSD) for the averaged element

concentrations of the single spot measurements was <17 %, < 6 %, and < 11 % for NIST SRM 614 (n = 9), GSD-1G (n = 9), and BCR-2G (n = 6), respectively. The element concentrations measured on the QCM (APPENDIX_TABLE_1) agree within <13 % with preferred values for most elements, but As (30 % in GSD-1G), Sn (21 % in GSD-1G and BCR-2G), and Tl (18 % in NIST SRM 614). The difference between measured and true Tl concentration in NIST SRM 614 could be explained by analyses not only in the core region of the glass wafer but also closer to the rims. The rims have been reported to be depleted in some elements including Tl (Jochum et al. 2011).

During regular measurement conditions (sensitivities optimized for the full mass range), about 800 cps on $^{205}$Tl were measured per 1 µg/g Tl. For both Tl masses, background intensities are usually below 50 cps and relatively stable, resulting in minimum detection limits of about 0.2 µg/g. Isobaric interferences on the Tl masses appear to be of little importance, since the concentrations calculated from the intensities measured for $^{203}$Tl and $^{205}$Tl agree typically within 20 % for Tl concentrations >0.2 µg/g and within 3 % for Tl concentrations of >10 µg/g.

## Results

*Chemical composition of the sulfides and sulfosalts from the Lengenbach deposit*

The various samples from the Lengenbach deposit show a wide range of As concentrations (see Tab. 2) from 8.50 wt% in jordanite (Bin3) to 33.4 wt% in the sulfide melt inclusions (Bin13). This leads to molar (As+Sb)/S-ratios between 0.24 in jordanite to 0.51 in the sulfide melt inclusions (see Fig. 2a). The investigated samples also show a large range in Sb contents. The concentrations in the fahlore samples are low ranging from below the detection limit up to ~0.1 wt%. All other samples show higher contents from 0.32 wt% in the sulfide melt inclusions (Bin13) and up to >2 wt% in jordanite (Bin3). This leads to a broad range in molar As/Sb-ratios between 7 in jordanite (Bin3) and 169 in the sulfide melt inclusions (Bin13). Fahlores have even higher molar As/Sb-ratios between 312 (Bin5) and 794 (Bin2).

Some of the samples are rich in Pb and Tl. Pb contents reach up to 70 wt% in jordanite (Bin3). The highest concentration of Tl of 24.8 wt% was determined in hatchite (Bin4). However, some of the samples have Pb and Tl abundances below the detection limit (both ~200 µg/g, depending on the minerals analyzed) and especially the fahlores do not show measurable contents of these elements. As a consequence, molar Pb/Tl-ratios, where they could be obtained, vary between 0.99 in edenharterite (Bin3) and 581 in jordanite (Bin6; see Fig. 2b).

The sulfosalts from the Lengenbach quarry show a large range in molar Tl/As-ratios. Fahlore samples have the lowest molar Tl/As-ratios of 0.001 (Bin2). Other sulfosalts have molar Tl/As-ratios ranging from 0.004 in sartorite (Bin9) to 0.56 in hatchite (Bin4).

The fahlore samples (Bin2 and Bin5) are tennantites with high Cu and Zn contents between 42.0 to 42.9 wt% and 8.23 to 8.55 wt%, respectively. The contents of Fe are low (between 0.17 wt% and 0.25 wt%), while the Ag contents are rather high with concentrations between 1.32 wt% and 1.59 wt%. No Bi could be detected in our samples (see Fig. 3b).

*Chemical composition of the sulfide samples from Pizzo Cervandone*

The fahlores of the Cu-As mineralization at Pizzo Cervandone are also tennantites (see Tab. 2). In addition to As and S, we could detect Cu, Fe, Zn, Ag, Bi and Sb (see Fig. 3). The Cu contents are high and vary between 43.2 wt% and 43.7 wt%, but Zn (3.54 to 3.88 wt%) and Ag contents (0.18 to 0.28 wt%) are low. Iron (3.89 to 4.13 wt%) and Bi (1.07 to 1.31 wt%) occur in significant concentrations. The contents of Sb are within a narrow range between 0.30 and 0.33 wt%. This leads to low molar As/Sb-ratios between 94 and 104.

*Trace elements in fissure micas*

The Tl contents of dolomite-hosted micas (Table 3, Fig. 4) show a large variation from 1.91 µg/g

(Bin21) to 346 µg/g (Bin18). Micas from the Feldbacher stratum (Bin24, Bin30) have relatively limited Tl concentrations between 2.51 µg/g (Bin30) and 7.34 µg/g (Bin24), and the sample from Balmen is characterized by a Tl abundance of 8.11 µg/g (Bin23; see Fig. 4). In contrast, mica samples from the Lengenbacher stratum (Bin16, Bin18, Bin19, Bin21) are the most variable ones with regard to Tl concentrations (values from 1.91 to 346 µg/g). Micas hosted by granitic gneisses are restricted to Tl contents between 2.10 µg/g (Bin28) and 20.04 µg/g (Bin22). Arsenic abundances are mostly below the detection limit, whereas concentrations can reach high levels up to 79.6 µg/g in sample Bin26. All micas with measurable contents of As are from orthogneiss host rocks.

The Rb contents range from 259 µg/g (Bin21) to 2534 µg/g (Bin22). The concentrations of Rb show a continuum, but three groups can be distinguished based on their host rocks. Samples hosted by Lengenbach strata dolomites generally show lower Rb contents (up to 375 µg/g for Bin18) than the other samples hosted by dolomites. The samples hosted by dolomites have Rb contents between 349 and 432 µg/g (both Bin30), these are lower than Rb concentrations in samples hosted by orthogneisses (>447 µg/g in Bin25). The Cs contents show similar systematics: the samples from the dolomite of the Lengenbacher stratum have Cs concentrations between 6.33 µg/g (Bin16) and 13.7 µg/g (Bin21), whereas samples hosted by the Feldbach stratum show Cs contents from 6.37 µg/g (Bin30) to 142 µg/g (Bin24). Micas hosted by granitic gneisses are also relatively rich in Cs (values from 6.82 µg/g in Bin28 to 523 µg/g in Bin22).

*Isotope composition of Tl*

The Tl isotope compositions were determined for ten samples from Lengenbach, three from Pizzo Cervandone and two from Wiesloch. These data (see Tab. 4) show a broad range of values between $\varepsilon^{205}Tl$ = -4.1 (Bin1) and +1.9 (Bin6). Both extreme results are from samples of the Lengenbach deposit demonstrating the high variability within this deposit (Fig. 5). At Lengenbach, jordanite is the mineral species with the lightest isotope compositions between $\varepsilon^{205}Tl$ = -4.1 and -1.5. One

sartorite sample is isotopically heavier than jordanite, but another sartorite sample is slightly lighter with a value of $\varepsilon^{205}$Tl = -2.2. The other sulfosalts have higher values ranging from $\varepsilon^{205}$Tl = +0.6 to +1.9 whilst the sulfide melt inclusions shows $\varepsilon^{205}$Tl = -0.3. The Tl isotope composition of the arsenite sample (asbecasite; $\varepsilon^{205}$Tl = -2.0) from the Cu-As mineralization at Pizzo Cervandone falls right in the range of the fahlore compositions from the same locality ($\varepsilon^{205}$Tl = -3.0 and 0.1). The samples from the Wiesloch deposit show a smaller but still significant isotopic variability with $\varepsilon^{205}$Tl values between -1.4 and -2.7.

## Discussion

The formation of the Lengenbach deposit has been explained by melting of a stratabound precursor mineralization of pre-Alpine age (Hofmann 1994). The Alpine metamorphism caused the melting, and a subsequent fractional crystallization of the sulfide melt lead to the formation of the observed large variety of sulfosalts.

The assumption of a stratabound precursor mineralization is based on the observation that the mineralization in Lengenbach only occurs in metamorphosed Triassic dolomites. The association of dolomites with sulfide mineralization is typical of Mississippi Valley-type deposits known from several localities in Triassic dolomites such as e.g. Bleiberg, Austria, and Meggen and Wiesloch, Germany (Gasser 1974; Gasser and Thein 1977; Schroll 1996; Pfaff et al. 2010).

### *The precursor mineralization and implications on external sources*

The elemental inventory of the Mississippi Valley-type deposits mentioned above is rather similar to what is found in the Lengenbach deposit (Hofmann and Knill 1996). The Tl isotope composition of sulfides from the Wiesloch deposit ($\varepsilon^{205}$Tl of -1.4 and –2.7) is also isotopically similar to the composition of the Lengenbach deposit (Fig. 5). However, since our dataset is unfortunately too limited to draw the conclusion if an external elemental input has occurred.

Even if the elemental inventory of Lengenbach is similar to the deposits discussed above, typical Mississippi Valley-type deposits show lower As/Sb-ratios than the Lengenbach deposit (Hofmann and Knill 1996). This can be explained by the addition of As to the Lengenbach deposit by hydrothermal fluids before or during Alpine metamorphism (Graeser and Roggiani 1976). Arsenic could principally be derived from Cu-As mineralizations located in basement orthogneisses as e.g. at Pizzo Cervandone. This model would also explain the high Cu contents of Lengenbach compared to Mississippi Valley-type deposits like Wiesloch. Mobilization of As at Pizzo Cervandone is corroborated by the abundant occurrence of As-bearing minerals in nearby Alpine fissures (Graser and Roggiani 1976; Guastoni et al. 2006).

The ionic radii as well as the charge of Tl and Rb are very similar, which implies that the partitioning into mica is constant. Therefore, Rb/Tl-ratios in micas can be used as proxy for the fluids crystallizing mica. However, based on the Rb-Tl systematics of micas both in host rocks, their fissures and in the Lengenbach deposit (Fig. 4), no influence of an external fluid can be discerned. Fissure micas of the mineralization in the Lengenbach dolomite stratum have compositions different from all other analyzed mica samples with respect to Tl and Rb (Fig. 4). This can be explained if Lengenbach is considered as a closed system during this fluid activity. The fluid activity recorded in the fissure micas occurred at the time of or after fissure formation. Sulfide melts, such as at Lengenbach (Hofmann 1994) are dominated by the components of sulfosalts which have low solidus temperatures down to 300 ºC (Tomkins et al. 2007). This is 200 ºC lower than peak metamorphic temperatures in the Binntal area and it also means that the crystallization interval of the sulfide melt from liquidus to complete solidification is unusually large (>200 ºC) (Tomkins et al. 2007). This 200 ºC cooling from about 500 to about 300 °C probably took around 20 Ma (Challandes et al. 2008) which in turn had the effect that the melt could interact with hydrothermal fluids (e.g. with those present during the crystallization of the fissure micas). We propose that in this temperature interval, the fissures and their micas could be formed and hence

could have reacted and equilibrated with the sulfide melt present in the rocks. In agreement with this statement, the fissure micas from the Lengenbach deposit show higher Tl contents than any other mica samples, indicating a very Tl-rich hydrothermal environment already during mica growth.

Based on the distinct and relatively low Rb/Tl ratios of micas from the Lengenbach deposit (Fig. 4), we again conclude that either the precursor sulfide mineralization was already enriched in Tl or the enrichment took place under near-peak metamorphic conditions. Under peak metamorphic conditions the sulfide melt could have interacted with hydrothermal fluid and element scavenging could have effectively enriched the sulfide melt in Tl and As (Tooth et al. 2011). In contrast, fissure micas from dolomites of the Feldbacher stratum have higher concentrations of Rb than samples from the Lengenbacher stratum. The hydrothermal fluid responsible for the crystallization of the fissure micas might have been influenced by the Bündnerschiefer surrounding the Feldbacher dolomite stratum. Fissure micas from basement orthogneisses show Rb and Tl contents similar to granitic crustal rocks (Rudnick and Gao 2003). In these fissures, also the arsenite minerals occur recording the mobilization of the Pizzo Cervandone mineralization. Interestingly, and importantly, however, they do not record at all the presence of a Tl-rich hydrothermal fluid.

The Tl isotope composition of most minerals from the Lengenbach deposit is heavier than the average crustal value of $\varepsilon^{205}Tl \approx -2$ (Fig. 5; Nielsen et al. 2005; Nielsen et al., 2011). The only reservoir known to contain very heavy isotope compositions of Tl are marine ferromanganese (Fe-Mn) oxides (Rehkämper et al., 2002; Rehkämper et al., 2004; Nielsen et al. 2009). In agreement with investigations of Hofmann and Knill (1996), sea floor oxides, such as Fe-Mn nodules, are among possible Lengenbach precursor rocks and hence they might have contributed to the element inventory of the deposit, although we admit that it is not typical to find such nodules on carbonate platforms. In addition, Fe-Mn oxides can be highly enriched in Tl (Rehkämper et al., 2002; Rehkämper et al., 2004) and, therefore, are able to exert a major control on the Tl budget of the

Lengenbach deposit. The conclusion that marine Fe-Mn oxides can dominate the Tl budget of magmatic systems is in accordance with a previous study, which suggested that the relatively high $\varepsilon^{205}$Tl of some Hawaiian magmas is also a signature of such materials (Nielsen et al. 2006). As shown by Calvert and Price (1977) and by Neal et al. (1979), such sea-floor oxides also contain significant amounts of As and Cu. Accordingly, we propose that the precursor of the Lengenbach mineralization may have been chemically modified by the addition of Tl, Cu and As from sea-floor fluids and related Mn-oxides. The only other source for Tl could be K- (and therefore Tl-) bearing minerals in the surrounding host rocks such as micas in the Bündnerschiefer or K-feldspar in the granitic gneisses.

*Evidence from Tl isotope composition on the origin and mobilization of the Pizzo Cervandone mineralization*

The Tl isotope composition of the mineralization at Pizzo Cervandone (Fig. 5) lies in the range previously determined for Cu porphyry deposits (Baker et al. 2010). This supports the interpretation of the magmatic origin of the Pizzo Cervandone mineralization as previously suggested by Graeser and Roggiani (1979). The isotopic composition of asbecasite from Alpine fissures at Pizzo Cervandone lies right in the middle of the range of the primary fahlores, indicating that a mobilization of "primary Tl" is assumed to have occurred during the Alpine metamorphism. However, the large range in the Tl isotopic composition of the primary minerals does not allow an evaluation of whether isotopic fractionation occurred during the alteration and mobilization process.

*Chemical and isotopic fractionation of the sulfide melt*

The range in the isotope composition of Tl within the Lengenbach deposit is 5 ε-units, which is large (Nielsen and Rehkämper 2011), especially for high-temperature processes (Schauble 2004). This large range can be theoretically explained by isotope fractionation during melt formation,

during fractional crystallization of the ore minerals from the melt, or by the input of variable amounts of Tl from sources with different isotope compositions. During fractional crystallization Tl and As are incompatible and enriched in the remaining melt fractions (Tomkins et al. 2007). This is also seen in the crystallization sequence of the Lengenbach deposit, where later As-rich minerals such as baumhauerite replace earlier As-poor phases such as e.g. jordanite (Giusca 1930). Comparing molar Tl/As-ratios of the analyzed minerals with their Tl isotope composition, we observe the lightest isotope compositions in the samples with the lowest molar Tl/As-ratios, and vice versa for phases with heavier Tl isotope compositions (Fig.6). This can be explained by the preferred incorporation of the lighter Tl isotope into the solid phase and an enrichment of the heavier isotope in the remaining sulfide melt if fractional crystallization is the most important process. In general, Tl isotope fractionation between sulfides or sulfosalts and a sulfide melt is thought to be small because S and As are the most important nearest structural neighbors in both cases. However, the structural arrangements (coordination and atomic distances) of these elements differ between minerals and melt, which might explain larger fractionation effects on Tl isotopes (compare e.g. Takeushi and Sadanaga 1969 and Pohl 1982). Larger fractionation is more likely for partitioning between a sulfide melt and an aqueous fluid, because the chemical environments are very different. Thallium is transported as a chloride complex in saline fluids (Xiong 2007), whereas it is probably ionic in the melt. The presence of a saline aqueous fluid at Lengenbach during and after the presence of the sulfide melt has been detected by the occurrence of fluid inclusions in quartz (Hofmann and Knill 1996). Accordingly, an isotopic equilibrium between solids, sulfide melt and an associated aqueous fluid can be assumed. In this case, isotope fractionation can be considered as a fractionation between a bulk mobile phase (i.e., melt plus aqueous fluid) and the solids, since isotope compositions shift due to mass-balance in the whole system. This model requires that sulfides incorporate more light isotopes compared to the aqueous fluid, resulting in a heavier bulk isotope composition of sulfide melt and aqueous fluid. This scenario could explain

most of the observed isotope variations.

The fahlores are the only minerals from the Lengenbach deposit, which do not follow the trend of increasing Tl/As-ratios with increasing $\varepsilon^{205}$Tl (Fig. 6). According to their Tl/As-ratio they should have crystallized at an early stage of the formation of the deposit. However, both the isotope composition of Tl and the As/Sb-ratios of the fahlores do not corroborate this (see Fig. 5). The isotope composition of Tl is among the heaviest found in the Lengenbach deposit suggesting a very late crystallization. The fact that fahlore falls off the general trend in the $\varepsilon^{205}$Tl vs. molar Tl/As-ratios diagram (Fig. 6) may reflect either that fahlore crystallization occurred after the sulfide melt had solidified, while hydrothermal activity persisted at lower temperature, or it may be a hint that indeed various metal sources contributed to the formation of the deposit.

Except for fahlore at Lengenbach, all of our results can be explained by Tl isotope fractionation occurring during fractional crystallization of a sulfide melt in equilibrium with an aqueous fluid. However, temperatures between 300 ºC and 500 ºC are very high for isotope fractionation of heavy elements such as Tl and cannot be caused by mass-dependent fractionation, which is very low at high temperatures (Bigeleisen and Mayer 1947). In contrast, nuclear volume-dependent or kinetic processes can cause significant fractionation at high temperatures. Nuclear volume-dependent fractionation is much stronger for heavy elements at high temperatures (Schauble 2007) and kinetic fractionation can be caused by differences in the activation energies of ongoing reactions. However, kinetic fractionation is dependent on the differences of ionic properties between the isotopes or on diffusivity in high temperature processes (Schauble 2004). Since the mass difference is small and diffusivity is rapid in sulfide melts (Majewsky and Walker 1998), this process probably is minor, unless unknown kinetic effects take place.

## Implications

Our study shows that crystallization of a sulfide melt can cause fractionation of heavy elements, as

450 exemplified by Tl. Therefore the isotopic analysis of high-temperature mineral deposits can be used
451 trace element distribution in a metamorphic environment where sulfide melts form. The
452 crystallization products of metamorphic sulfide melts form some world-class mineral deposits, and
453 isotopic investigations might give further hints on their generation and the processes involved.
454

455 **Acknowledgments**

456 We thank T. Raber, S. Graeser and B. Hofmann for providing sample material, and I. Gill-Kopp for
457 sample preparation. Financial support of this study has been provided by the
458 Landesgraduiertenförderung Baden-Württemberg to Kai Hettmann. We also like to thank S.Nielsen
459 and J. Brugger for their constructive reviews, which helped to improve this manuscript.
460

461 **References**

462 Armbruster, T., Bühler, C., Graeser, St., Stalder, H. A., and Amthauer, G. (1988) Cervandonite-(Ce),
463 (Ce,Nd,La)(Fe3+,Fe2+,Ti4+,Al)3SiAs(Si,As)O13, a new Alpine fissure mineral. Schweizerische
464 Mineralogische und Petrographische Mitteilungen, 68, 125-132.
465 Baker, R.G.A., Rehkämper, M., Ihlenfeld, C., Oates, C.J., and Coggon, R. (2010) Thallium isotope
466 variations in an ore-bearing continental igneous setting: Collahuasi Formation, northern Chile.
467 Geochimica et Cosmochimica Acta, 74, 4405-4416.
468 Baker R. G. A., Rehkämper M., Hinkley T. K., Nielsen S. G. and Toutain J. P. (2009) Investigation
469 of thallium fluxes from subaerial volcanism—implications for the present and past mass balance of
470 thallium in the oceans. Geochimica et Cosmochimica Acta 73, 6340–6359.
471 Bigeleisen, J. and Mayer, M. G. (1947) Calculation of equilibrium constants for isotopic exchange
472 reactions. Journal of Chemical Physics 15, 261–267.
473 Calvert, S.E. and Price, N.B. (1977) Geochemical Variation in Ferromanganese Nodules and
474 Associated Sediments from the Pacific Ocean. Marine Chemistry, 5, 43-74.

475 Challandes, N., Marquer, D., and Villa, I.M. (2008) P-T-t modelling, fluid circulation, and 39Ar-
476 40Ar and Rb-Sr mica ages in the Aar Massif shear zones (Swiss Alps). Swiss Journal of
477 Geosciences 101, 269-288.
478 Demartin, F., Gramaccioli, C. M., and Pilati, T. (1994) Paraniite-(Y), a new tungstate arsenate
479 mineral from Alpine fissures. Schweizerische Mineralogische und Petrographische Mitteilungen,
480 74, 155-160.
481 Frey, M., Hunziker, J.C., Frank, W., Bocquet, J., Dal Piaz, G.V., Jäger, E., and Niggli, E. (1974)
482 Alpine metamorphism of the Alps. A review. Schweizerische Mineralogische und Petrographische
483 Mitteilungen, 54, 247-290.
484 Galster, F., Cavargna-Sani, M., Epard, J-L., and Masson, H. (in press) New stratigraphic data from
485 the Lower Penninic between the Adula nappe and the Gotthard massif and consequences for the
486 tectonics and the paleogeography of the Central Alps. Tectonophysics, in press.
487 Gasser, U. (1974) Zur Struktur und Geochemie der stratiformen Sulfidlagerstätte Meggen
488 (Mitteldevon, Rheinisches Schiefergebirge). Geologische Rundschau 63, 52-73
489 Gasser, U. and Thein, J. (1977) Das syngenetische Sulfidlager Meggen im Sauerland (Struktur,
490 Geochemie, Sekundärdispersion). Forschungsbericht des Landes Nordrhein-Westfalen No.
491 2620/Fachgruppe Chemie. Westdeutscher Verlag, 171 pp. (in German).
492 Giusca, D. (1930) Die Erze der Lagerstätte vom Lengenbach im Binnental (Wallis). Schweizerische
493 Mineralogische und Petrographische Mitteilungen, 10, 152-177 (in German).
494 Graeser, S. (1965) Die Mineralfundstellen im Dolomit des Binnatales. Schweizerische
495 Mineralogische und Petrographische Mitteilungen, 45, 597-795 (in German).
496 Graeser, S. (1975) Die Mineralfundstelle Lengenbach, Binntal. Schweizerische Mineralogische und
497 Petrographische Mitteilungen, 55, 143-149 (in German).
498 Graeser, S. and Roggiani, A. G. (1976) Occurrence and genesis of rare arsenate and phosphate
499 minerals around Pizzo Cervandone, Italy/Switzerland. Rendicontri della Societa Italiana di

Mineralogia e Petrologia, 32, 279-288.

Graeser, S., Schwander, F., Gramaccioli, C.M., Pilati, T., and Reusser, E. (1994) Fetiasite (Fe2+, Fe3+,Ti)3O2[As2O5], a new arsenite mineral; its description and structure determination. American Mineralogist, 79, 996-1002.

Graeser, S., Cannon, R., Drechsler, E., Roth, P., and Raber, T. (2008) Faszination Lengenbach, Abbau – Forschung – Mineralien (1958-2008). Kristallografik Verlag, Achberg (in German).

Guastoni, A., Pezzota, F., and Vignola, P. (2006) Characterization and genetic inferences of arsenates, sulfates and vanadates of Fe, Cu, Pb, Zn from Mount Cervadone (Western Alps, Italy). Periodico di Mineralogia, 75, 141-150.

Hofmann, B. (1994) Formation of a sulfide melt during Alpine metamorphism of the Lengenbach polymetallic sulfide mineralization, Binntal, Switzerland. Mineralium Deposita, 29, 439-442.

Hofmann, B. and Knill, M.D. (1996) Geochemistry and genesis of the Lengenbach Pb-Zn-As-Tl-Ba-mineralisation, Binn Valley, Switzerland. Mineralium Deposita, 31, 319-339.

Hofmann, B., Graeser, S., Imhof, T., Sicher, V., and Stalder, H.A. (1993) Mineralogie der Grube Lengenbach, Binntal, Wallis. Jahrbuch des Naturhistorischen Museums Bern, 11, 3-90 (in German).

Jochum, K.P., Nohl, U., Herwig, K., Lammel, E., Stoll, B., Hofmann, A.W. (2005) GeoReM: a new geochemical database for reference materials and isotopic standards. Geostandards and Geoanalytical Research 29, 333–338.

Jochum, K.P. , Weis, U., Stoll, B.,. Kuzmin, D., Yang, Q., Raczek, I., Jacob, D.E., Stracke, A., Birbaum, K. ,Frick, D.A., Günther, D., and Enzweiler, J. (2011) Determination of reference values for NIST SRM 610-617 glasses following ISO guidelines. Geostandards and Geoanalytical Research, 35, 397-429

Majewski, E., and Walker, D. (1998) S diffusivity in Fe–Ni–S–P melts. Earth and Planetary Science Letters 160, 823-830.

Neal, C., Elderfield, H., and Chester, R. (1979) Arsenic in Sediments of the North Atlantic Ocean

525 and the Eastern Mediterranean Sea. Marine Chemistry, 7, 207-219.
526 Nielsen, S.G., Rehkämper, M., Porcelli, D., Andersson, P. Halliday, A.N., Swarzenski, P.W.,
527 Latkoczy, C., and Günther, D. (2005) Thallium isotope composition of the upper continental crust
528 and rivers – An investigation of the continental sources of dissolved marine Thallium. Geochimica
529 et Cosmochimica Acta, 19, 2007-2019.
530 Nielsen, S.G., Rehkämper, M., Norman, M.D., Halliday, A.N., and Harrison, D. (2006) Thallium
531 isotopic evidence for ferromanganese sediments in the mantle source of Hawaiian basalts. Nature
532 439, 314-317.
533 Nielsen, S.G. and Rehkämper, M. (2011) Thallium isotopes and their application to problems in
534 earth and environmental science. In: Handbook of environmental isotope geochemistry. Springer
535 Berlin Heidelberg. 247-269.
536 Nielsen, S. G. and Lee, C.-T. A. (2013), Determination of Thallium in the USGS Glass Reference
537 Materials BIR-1G, BHVO-2G and BCR-2G and Application to Quantitative Tl Concentrations by
538 LA-ICP-MS. Geostandards and Geoanalytical Research. doi: 10.1111/j.1751-908x.2012.00203.x
539 Nielsen, S.G., Mar-Gerrison, S., Gannoun, A., LaRowe, D., Klemm, V., Halliday, A. N., Burton, K.
540 W., and Hein, J. R. (2009) Thallium Isotope Evidence for Increased Marine Organic Carbon Export
541 in the Early Eocene. Earth and Planetary Science Letters, 278, 297-307.
542 Pfaff, K., Hildebrandt, L. H., Leach, D. L., Jacob, D. E., and Markl, G. (2010). Formation of the
543 Wiesloch Mississippi Valley-type Zn-Pb-Ag deposit in the extensional setting of the Upper
544 Rhinegraben, SW Germany. Mineralium Deposita, 45, 647-666.
545 Pohl, K.D. (1982) Orientation birefringence and structure of sulfur and arsenic sulfide melts.
546 Physics and Chemistry of Glasses, 23, 23-30.
547 Rehkämper, M. and Halliday, A.N. (1998) The precise measurement of Tl isotopic compositions by
548 MC-ICPMS: Application to the analysis of geological materials and meteorites. Geochimica et
549 Cosmochimica Acta, 63, 935–944.

550 Rehkämper, M., Frank, M., Hein, J.R., Porcelli, D., Halliday, A.N., Ingri, J., Liebetrau, V., 2002.
551 Thallium isotope variations in seawater and hydrogenetic, diagenetic, and hydrothermal
552 ferromanganese deposits. Earth Planet. Sci. Lett. 197, 65-81.
553 Rehkämper, M., Frank, M., Hein, J.R., Halliday, A.N., 2004. Cenozoic marine geochemistry of
554 thallium deduced from isotopic studies of ferromanganese crusts. Earth Planet. Sci. Lett. 219, 77-
555 91.
556 Rudnick, R.L. and Gao, S. (2003) The Composition of the Continental Crust, 1-64. In: The Crust
557 (ed. R.L. Rudnick) Vol. 3, Treatise on Geochemistry (eds. H.D. Holland and K.K. Turekian),
558 Elsevier-Pergamon, Oxford.
559 Schauble, E. (2004) Applying Stable Isotope Fract6ionation Theory to New Systems. Reviews in
560 Mineralogy and Geochemistry 55, 65-111.
561 Schauble, E.I. (2007) Role of nuclear volume in driving equilibrium stable isotope fractionation of
562 mercury, thallium, and other very heavy elements. Geochimica et Cosmochimica Acta, 71, 2170 -
563 2189.
564 Schroll E. (1996) The Triassic carbonate-hosted Pb-Zn mineralization in the Alps (Europe): The
565 genetic position of Bleiberg type deposits. In: Sangster D.F. (ed.) Carbonate-hosted lead-zinc
566 deposits. Society of Economic Geology Special Publications, 4, 182–194.
567 Sparks, H.A. and Mavrogenes, J.A. (2005) Sulfide melt inclusions as evidence for the existence of a
568 sulfide partial melt at Brocken Hill, Australia. Economic Geology, 100, 773-779.
569 Staude, S., Mordhorst, T., Neumann, R., Prebeck, W., and Markl, G. (2010). Compositional variation
570 of the tennantite–tetrahedrite solid-solution series in the Schwarzwald ore district (SW Germany):
571 The role of mineralization processes and fluid source. Mineralogical Magazine, 74, 309-339.
572 Takeuchi, Y., and Sadanaga, R. (1969). Structural principles and classification of sulfosalts.
573 Zeitschrift für Kristallographie, 130, 346-368.
574 Tomkins, A.G., Pattison, D.R.M., and Frost B.R. (2007) On the initiation of metamorphic sulfide

anatexis. Journal of Petrology, 48, 511-535.

Tooth, B., Ciobanu, C., Neil, B., Green, L., and Brugger, J. (2011) Bi-melt formation and Gold scavening from hydrothermal fluids: An experimental study. Geochimica et Cosmochimica Acta 75, 5423-5443.

Vance, D. and O'Nions, R.K. (1992) Prograde and retrograde thermal histories from the central Swiss Alps. Earth and Planetary Science Letters,114, 113-129.

Xiong, Y. (2007) Hydrothermal thallium mineralization up to 300°C: A thermodynamic approach. Ore Geology Reviews, 32, 291-313.

**Figure Captions**

Fig. 1 Schematic geological profile through the Binn Valley, Switzerland, showing the location of the Lengenbach quarry and the Pizzo Cervandone deposit.

Fig. 2 The composition of sulfosalts from the Lengenbach quarry. (a) molar As/Sb vs. molar (As+Sb)/S; (b) molar Pb/Tl vs. molar (As+Sb)/S.

Fig. 3 The composition of fahlore from the Lengenbach and the Pizzo Cervandone deposits. (a) Cu+Fe vs. Ag+Zn; (b) ternary molar composition in the As-Bi-Sb system.

Fig. 4 Rb vs. Tl contents of fissure micas. Crustal Rb/Tl-ratios have been taken from Rudnick & Gao (2003)

Fig. 5 The Tl isotope composition of various minerals from the Lengenbach quarry, Pizzo Cervandone and the Wiesloch deposits.

Fig. 6 Thallium isotope composition of sulfosalts from the Lengenbach quarry plotted versus molar Tl/As-ratios

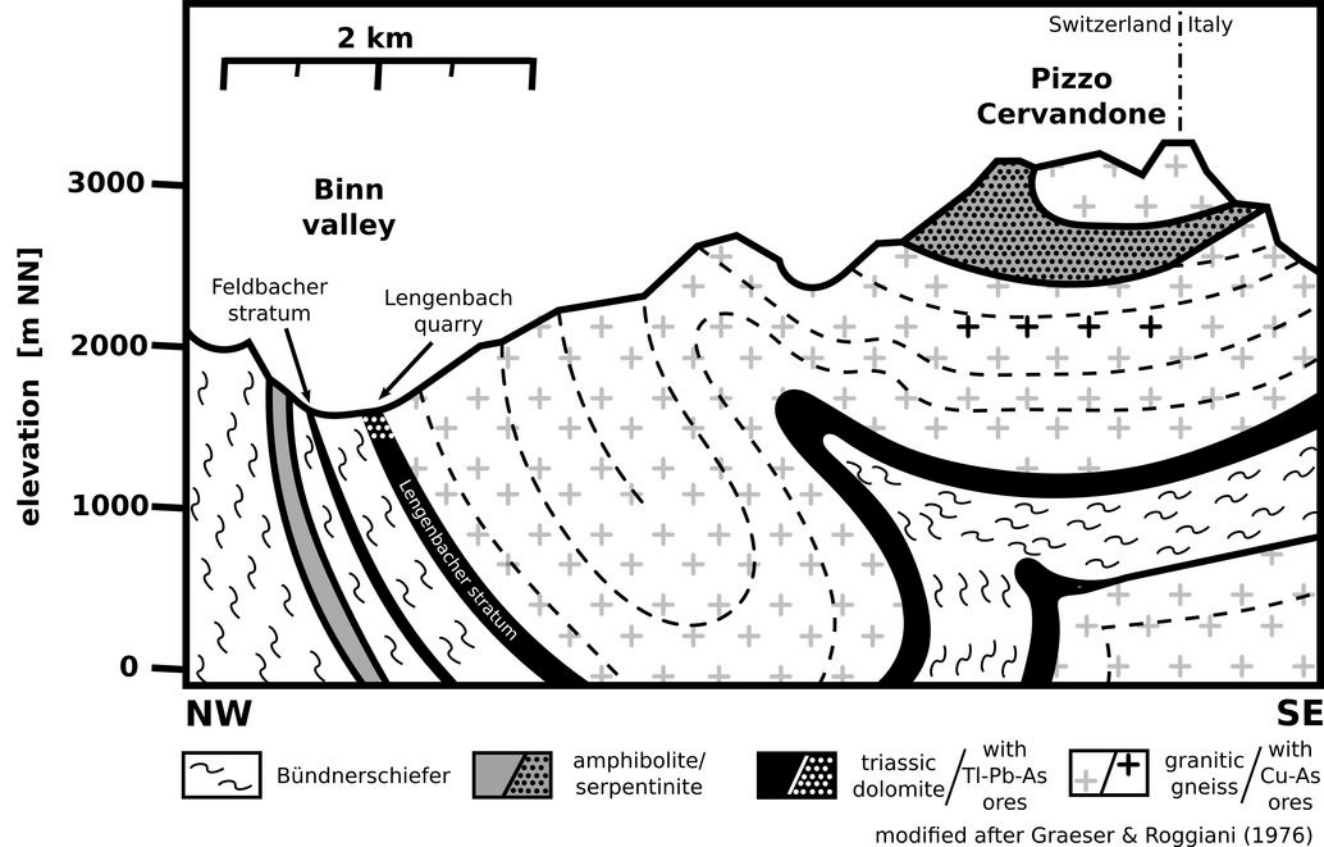
2 km
Switzerland
Italy
Pizzo
Cervandone
Binn
valley
3000
2000
1000
0
elevation [m NN]
Feldbacher
stratum
Lengenbach
quarry
Lengenbacher stratum
NW
SE
Bündnerschiefer
amphibolite/
serpentinite
triassic
dolomite
with
Tl-Pb-As
ores
granitic
gneiss
with
Cu-As
ores
modified after Graeser & Roggiani (1976)

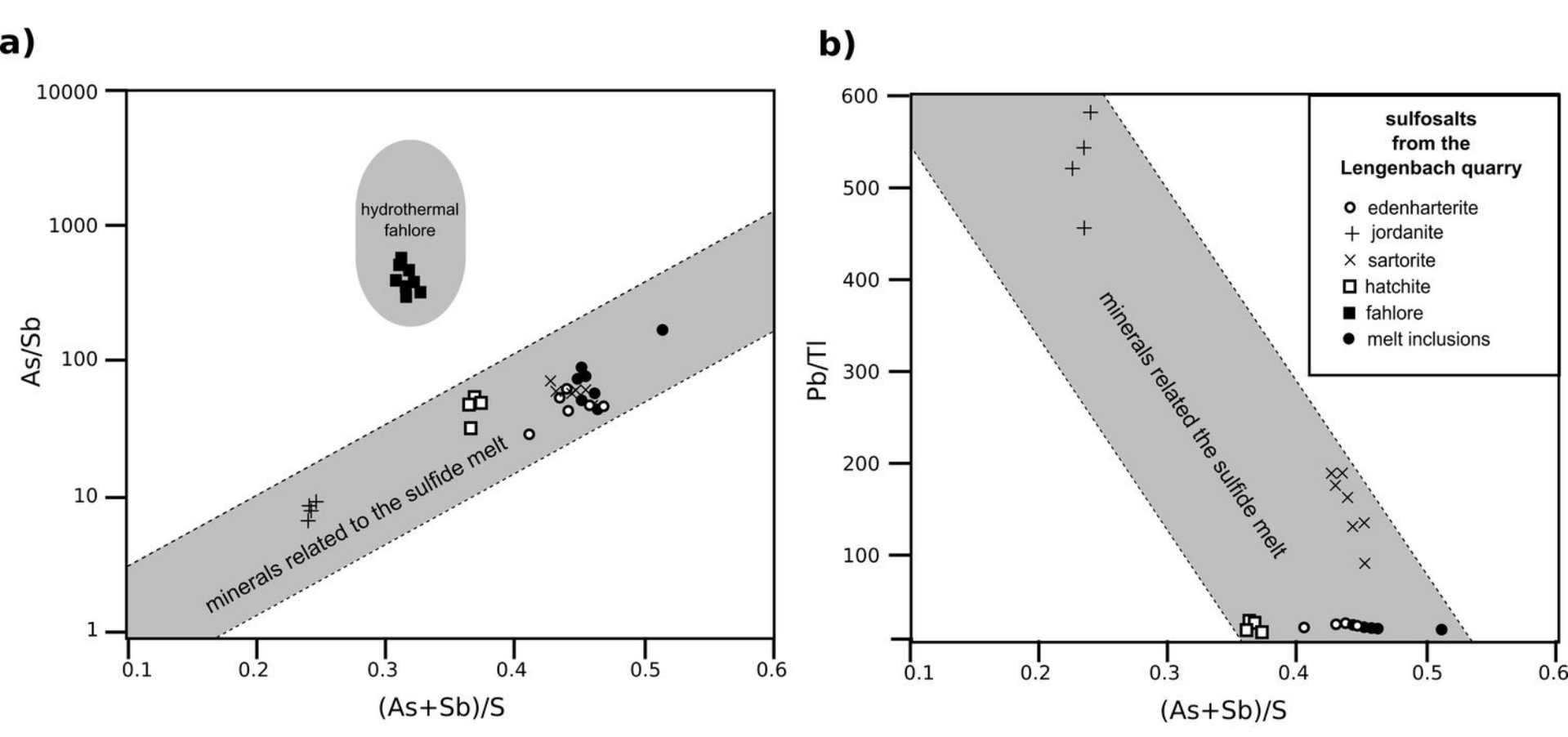
a)
b)
hydrothermal fahlore
minerals related to the sulfide melt
As/Sb
(As+Sb)/S
Pb/Tl
sulfosalts from the Lengenbach quarry
edenharterite
jordanite
sartorite
hatchite
fahlore
melt inclusions

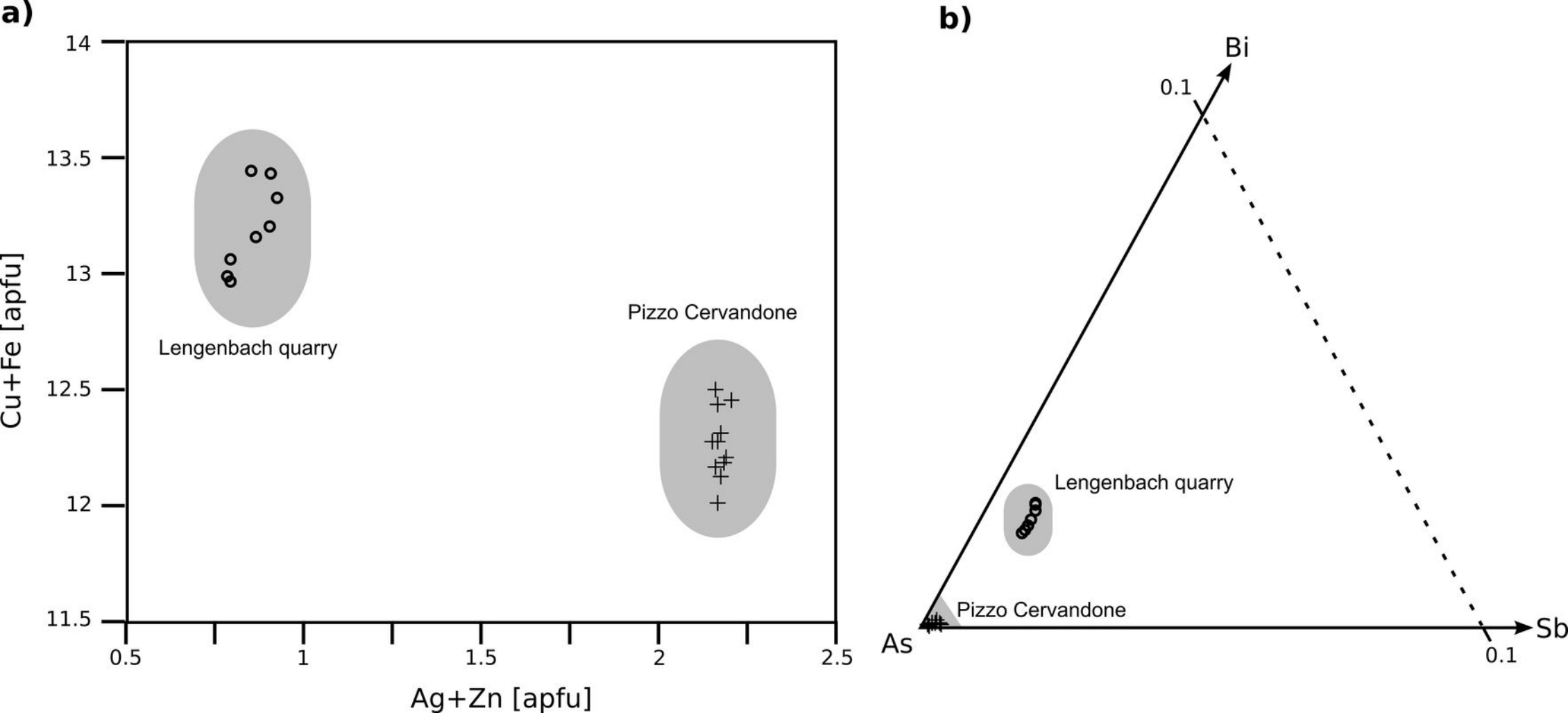
a)
14
13.5
13
12.5
12
11.5
Cu+Fe [apfu]
0.5
1
1.5
2
2.5
Ag+Zn [apfu]
Lengenbach quarry
Pizzo Cervandone
b)
Bi
0.1
Lengenbach quarry
Pizzo Cervandone
As
Sb
0.1

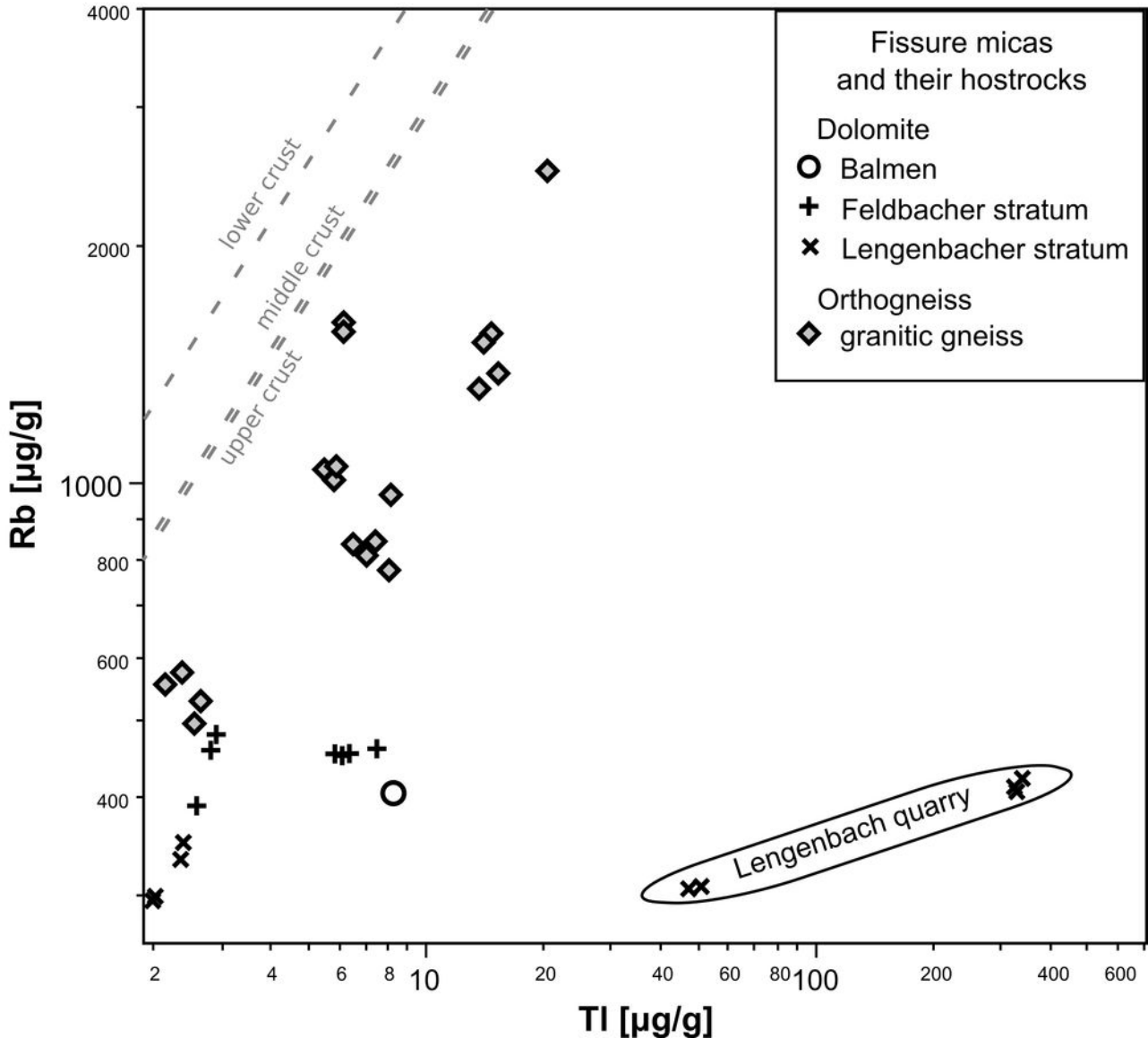
Fissure micas
and their hostrocks
Dolomite
Balmen
Feldbacher stratum
Lengenbacher stratum
Orthogneiss
granitic gneiss
lower crust
middle crust
upper crust
Lengenbach quarry
Rb [µg/g]
Tl [µg/g]
4000
2000
1000
800
600
400
2
4
6
8
10
20
40
60
80
100
200
400
600

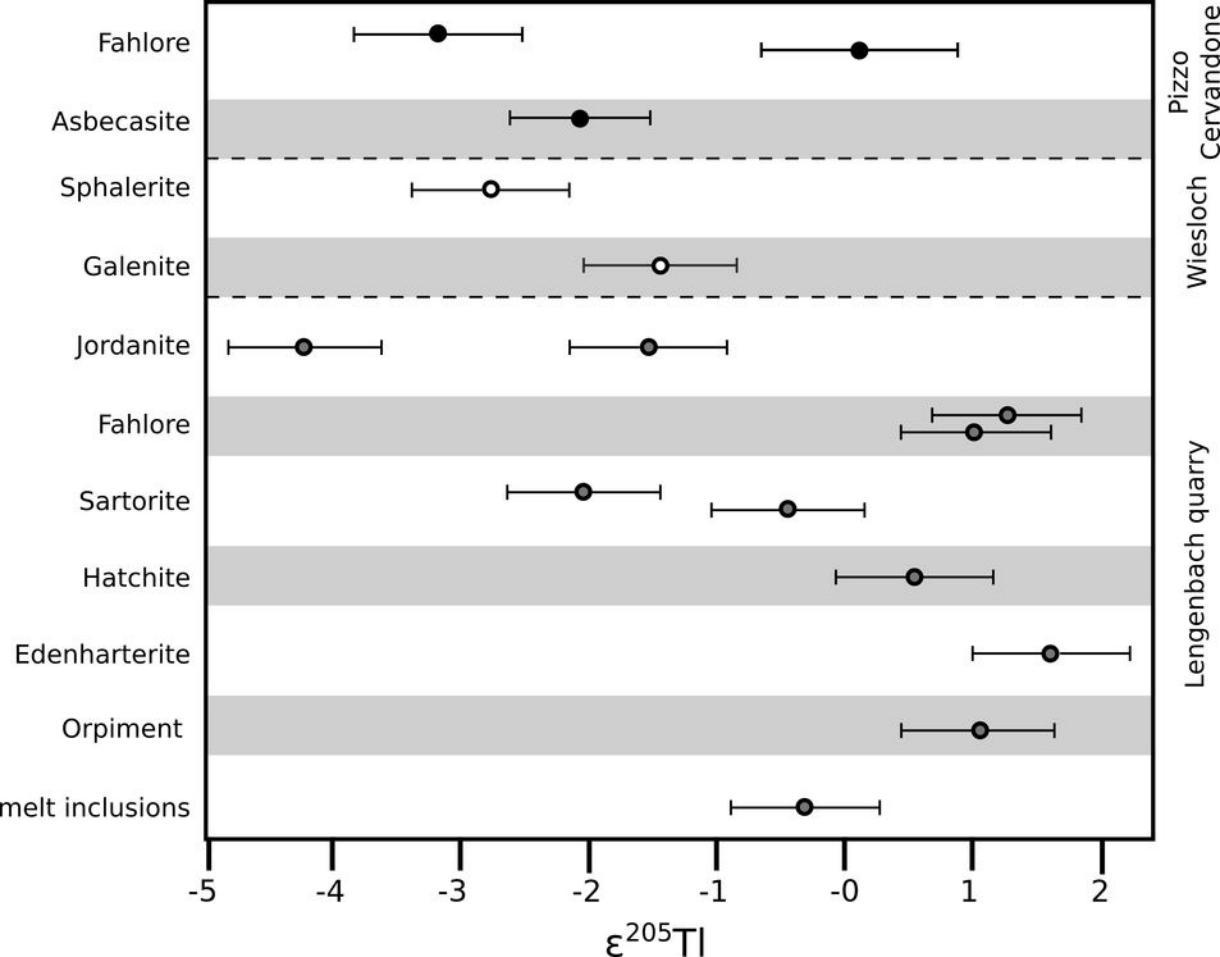
Fahlore
Asbecasite
Sphalerite
Galenite
Jordanite
Fahlore
Sartorite
Hatchite
Edenharterite
Orpiment
melt inclusions
Pizzo Cervandone
Wiesloch
Lengenbach quarry
-5
-4
-3
-2
-1
-0
1
2
ε205Tl

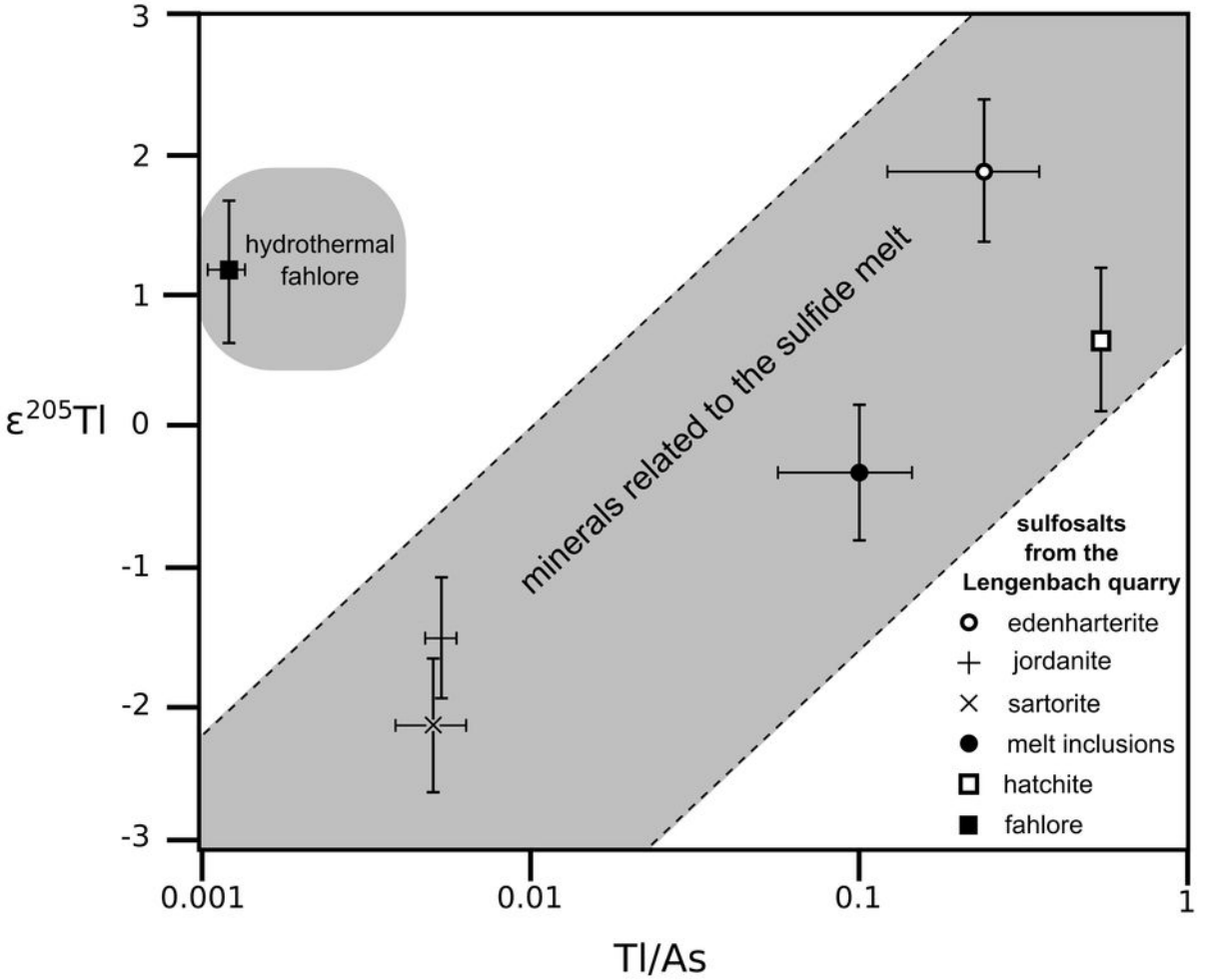
3
2
1
0
-1
-2
-3
ε205Tl
hydrothermal
fahlore
minerals related to the sulfide melt
sulfosalts
from the
Lengenbach quarry
edenharterite
jordanite
sartorite
melt inclusions
hatchite
fahlore
0.001
0.01
0.1
1
Tl/As

**Tab. 1 chemical composition of uncommon minerals mentioned in the text.**

| Mineral | Formula |
|---|---|
| asbecasite | $Ca_3TiAs_6Be_2Si_2O_{20}$ |
| baumhauerite | $Pb_{12}As_{16}S_{36}$ |
| cafarsite | $Ca_{5.9}Mn_{1.7}Fe_3Ti_3(AsO_3)_{12} \cdot 4\text{-}5H_2O$ |
| cervandonite-(Ce) | $(Ce,Nd,La)(Fe^{3+},Fe^{2+},Ti,Al)_3O_2(Si_2O_7)_{1-x+y}(As^{3+}O_3)_{1+x-y}(OH)_{3x-3y}$ |
| chalcopyrite | $FeCuS_2$ |
| dufrenoysite | $Pb_2As_2S_5$ |
| edenharterite | $PbTlAs_3S_6$ |
| fetiasite | $(Fe^{3+},Fe^{2+},Ti^{4+})_3(As_2O_5)O_2$ |
| galenite | PbS |
| gasparite-(Ce) | $(Ce,REE)AsO_4$ |
| giessenite | $(Cu,Fe)_2Pb_{26.4}(Bi,Sb)_{19.6}S_{57}$ |
| hatchite | $AgTlPbAs_2S_5$ |
| hutchinsonite | $(Tl,Pb)_2As_5S_9$ |
| jordanite | $Pb_{14}(As,Sb)_6S_{23}$ |
| molybdenite | $MoS_2$ |
| orpiment | $As_2S_3$ |
| paraniite-(Y) | $(Ca,Y,Dy)_2Y(WO_4)_2(AsO_4)$ |
| realgar | $As_4S_4$ |
| sartorite | $PbAs_2S_4$ |
| sphalerite | ZnS |
| tennantite | $Cu_6[Cu_4(Fe,Zn)_2]As_4S_{13}$ |

**Tab. 2 Major element composition of various sulfosalts**

| **Sample** | Bin6 | Bin6 | Bin6 | Bin6 | Bin6 | Bin6 | Bin6 | Bin4 | Bin4 | Bin4 | Bin4 |
|---|---|---|---|---|---|---|---|---|---|---|---|
| **Locality** | Lengenbach | Lengenbach | Lengenbach | Lengenbach | Lengenbach | Lengenbach | Lengenbach | Lengenbach | Lengenbach | Lengenbach | Lengenbach |
| **Mineral** | Edenharterite | Edenharterite | Edenharterite | Edenharterite | Edenharterite | Edenharterite | Edenharterite | Hatchite | Hatchite | Hatchite | Hatchite |
| **[wt% ]** | | | | | | | | | | | |
| **As** | 24.9 | 25.0 | 23.5 | 25.0 | 23.3 | 25.7 | 21.5 | 16.2 | 16.2 | 16.1 | 16.4 |
| **S** | 23.8 | 23.4 | 23.4 | 23.7 | 23.4 | 25.4 | 23.1 | 19.4 | 19.2 | 19.4 | 19.2 |
| **Tl** | 24.4 | 24.5 | 16.4 | 24.4 | 14.0 | 4.80 | 6.40 | 24.6 | 24.8 | 24.8 | 24.8 |
| **Mn** | 0.03 | 0.03 | 0.03 | 0.03 | bdl | bdl | bdl | bdl | bdl | bdl | 0.02 |
| **Sb** | 0.82 | 0.86 | 0.90 | 0.84 | 0.70 | 0.67 | 1.20 | 0.56 | 0.49 | 0.80 | 0.52 |
| **Bi** | bdl | bdl | bdl | bdl | bdl | bdl | bdl | bdl | bdl | bdl | bdl |
| **Cu** | 0.28 | 0.35 | bdl | 0.45 | 0.13 | 0.19 | bdl | 1.49 | 1.41 | 1.28 | 1.44 |
| **Ag** | bdl | bdl | 0.10 | bdl | 0.13 | 0.03 | 0.32 | 10.5 | 10.5 | 10.7 | 10.7 |
| **Zn** | bdl | 0.03 | bdl | bdl | bdl | bdl | bdl | bdl | bdl | bdl | 0.03 |
| **Pb** | 24.4 | 24.7 | 34.1 | 24.6 | 37.1 | 42.8 | 46.6 | 24.5 | 25.0 | 24.7 | 24.6 |
| **Fe** | 0.03 | bdl | bdl | bdl | bdl | 0.03 | 0.03 | bdl | bdl | bdl | bdl |
| **Total** | 98.7 | 98.8 | 98.5 | 99.0 | 98.8 | 99.7 | 99.1 | 97.3 | 97.7 | 97.8 | 97.7 |
| **[apfu]** | | | | | | | | | | | |
| **As** | 2.69 | 2.75 | 2.58 | 2.71 | 2.56 | 2.60 | 2.39 | 1.78 | 1.80 | 1.77 | 1.83 |
| **S** | 6 | 6 | 6 | 6 | 6 | 6 | 6 | 5 | 5 | 5 | 5 |
| **Tl** | 0.97 | 0.99 | 0.66 | 0.97 | 0.56 | 0.18 | 0.26 | 0.99 | 1.01 | 1.00 | 1.02 |
| **Mn** | 0.00 | 0.00 | 0.00 | 0.00 | | | | | | | 0.00 |
| **Sb** | 0.05 | 0.06 | 0.06 | 0.06 | 0.05 | 0.04 | 0.08 | 0.04 | 0.03 | 0.05 | 0.04 |
| **Bi** | | | | | | | | | | | |
| **Cu** | 0.04 | 0.05 | | 0.07 | 0.02 | 0.03 | | 0.23 | 0.22 | 0.20 | 0.22 |
| **Ag** | | | 0.01 | | 0.01 | 0.00 | 0.02 | 0.80 | 0.81 | 0.82 | 0.83 |
| **Zn** | | 0.00 | | | | | | | | | 0.00 |
| **Pb** | 0.95 | 0.98 | 1.35 | 0.96 | 1.47 | 1.56 | 1.87 | 0.98 | 1.01 | 0.98 | 0.99 |
| **Fe** | 0.00 | | | | | 0.00 | 0.00 | | | | |
| **(As+Sb)/S** | 0.46 | 0.47 | 0.44 | 0.46 | 0.43 | 0.44 | 0.41 | 0.36 | 0.37 | 0.37 | 0.37 |
| **As/Sb** | 50 | 47 | 42 | 48 | 54 | 63 | 29 | 47 | 54 | 33 | 51 |
| **Tl/As** | 0.36 | 0.36 | 0.26 | 0.36 | 0.22 | 0.07 | 0.11 | 0.56 | 0.56 | 0.56 | 0.56 |
| **Pb/Tl** | 0.99 | 0.99 | 2.05 | 1.00 | 2.61 | 8.80 | 7.17 | 0.98 | 1.00 | 0.98 | 0.98 |

**Tab. 2 Major element composition of various sulfosalts (continued)**

| **Sample** | Bin2 | Bin2 | Bin2 | Bin2 | Bin2 | Bin5 | Bin5 | Bin5 | Bin5 | Bin5 | Bin5 |
|---|---|---|---|---|---|---|---|---|---|---|---|
| **Locality** | Lengenbach | Lengenbach | Lengenbach | Lengenbach | Lengenbach | Lengenbach | Lengenbach | Lengenbach | Lengenbach | Lengenbach | Lengenbach |
| **Mineral** | Fahlore | Fahlore | Fahlore | Fahlore | Fahlore | Fahlore | Fahlore | Fahlore | Fahlore | Fahlore | Fahlore |
| **[wt%]** | | | | | | | | | | | |
| **As** | 19.8 | 19.9 | 20.2 | 20.0 | 19.9 | 20.1 | 20.2 | 20.1 | 20.2 | 19.8 | 19.8 |
| **S** | 27.2 | 27.5 | 27.4 | 27.3 | 27.1 | 26.7 | 27.3 | 26.8 | 27.2 | 27.3 | 26.8 |
| **Tl** | bdl | bdl | bdl | 0.06 | 0.07 | bdl | bdl | bdl | bdl | bdl | bdl |
| **Mn** | bdl | bdl | bdl | bdl | bdl | bdl | bdl | bdl | bdl | bdl | bdl |
| **Sb** | 0.06 | 0.06 | 0.07 | 0.04 | 0.09 | 0.10 | 0.07 | 0.09 | bdl | 0.08 | 0.10 |
| **Bi** | bdl | 0.08 | 0.08 | 0.02 | 0.08 | bdl | bdl | bdl | bdl | bdl | 0.01 |
| **Cu** | 42.9 | 42.6 | 42.7 | 42.6 | 42.5 | 42.7 | 42.0 | 42.7 | 42.6 | 42.5 | 42.8 |
| **Ag** | 1.42 | 1.59 | 1.36 | 1.35 | 1.47 | 1.32 | 1.40 | 1.41 | 1.37 | 1.50 | 1.36 |
| **Zn** | 8.41 | 8.40 | 8.53 | 8.55 | 8.27 | 8.23 | 8.44 | 8.38 | 8.33 | 8.35 | 8.27 |
| **Pb** | bdl | bdl | bdl | bdl | bdl | bdl | bdl | bdl | bdl | bdl | bdl |
| **Fe** | bdl | 0.24 | bdl | 0.20 | 0.25 | 0.22 | 0.20 | 0.25 | 0.24 | 0.24 | bdl |
| **Total** | 99.7 | 100.4 | 100.3 | 100.2 | 99.7 | 99.5 | 99.7 | 99.8 | 99.9 | 99.9 | 99.1 |
| **[apfu]** | | | | | | | | | | | |
| **As** | 4.05 | 4.02 | 4.11 | 4.08 | 4.09 | 4.19 | 4.11 | 4.17 | 4.15 | 4.04 | 4.09 |
| **S** | 13 | 13 | 13 | 13 | 13 | 13 | 13 | 13 | 13 | 13 | 13 |
| **Tl** | | | | 0.00 | 0.01 | | | | | | |
| **Mn** | | | | | | | | | | | 0.00 |
| **Sb** | 0.01 | 0.01 | 0.01 | 0.01 | 0.01 | 0.01 | 0.01 | 0.01 | | 0.01 | 0.01 |
| **Bi** | | 0.01 | 0.01 | 0.00 | 0.01 | | 0.00 | | | | 0.00 |
| **Cu** | 12.26 | 12.07 | 12.14 | 12.15 | 12.21 | 12.44 | 11.96 | 12.39 | 12.21 | 12.10 | 12.40 |
| **Ag** | 0.20 | 0.22 | 0.19 | 0.19 | 0.21 | 0.19 | 0.20 | 0.20 | 0.19 | 0.21 | 0.20 |
| **Zn** | 1.97 | 1.95 | 1.99 | 2.00 | 1.95 | 1.96 | 1.97 | 1.99 | 1.95 | 1.95 | 1.96 |
| **Pb** | | | | | | | | | | | |
| **Fe** | | 0.06 | | 0.05 | 0.07 | 0.06 | 0.06 | 0.07 | 0.07 | 0.07 | |
| **(As+Sb)/S** | 0.31 | 0.31 | 0.32 | 0.31 | 0.32 | 0.32 | 0.32 | 0.32 | 0.32 | 0.31 | 0.32 |
| **As/Sb** | 545 | 521 | 456 | 794 | 355 | 331 | 463 | 363 | | 398 | 312 |
| **Tl/As** | | | | 0.001 | 0.001 | | | | | | |
| **Pb/Tl** | | | | | | | | | | | |

**Tab. 2 Major element composition of various sulfosalts (continued)**

| **Sample** | Bin3 | Bin3 | Bin3 | Bin3 | Bin9 | Bin9 | Bin9 | Bin9 | Bin9 | Bin9 | Bin9 |
|---|---|---|---|---|---|---|---|---|---|---|---|
| **Locality** | Lengenbach | Lengenbach | Lengenbach | Lengenbach | Lengenbach | Lengenbach | Lengenbach | Lengenbach | Lengenbach | Lengenbach | Lengenbach |
| **Mineral** | Jordanite | Jordanite | Jordanite | Jordanite | Sartorite | Sartorite | Sartorite | Sartorite | Sartorite | Sartorite | Sartorite |
| **[wt%]** | | | | | | | | | | | |
| **As** | 8.66 | 8.90 | 8.78 | 8.50 | 23.0 | 25.6 | 24.5 | 24.8 | 22.7 | 24.6 | 22.8 |
| **S** | 17.2 | 17.1 | 17.3 | 17.4 | 23.0 | 24.3 | 23.4 | 24.2 | 22.9 | 24.0 | 23.2 |
| **Tl** | 0.13 | 0.12 | 0.15 | 0.13 | 0.27 | 0.59 | 0.38 | 0.37 | 0.30 | 0.31 | 0.28 |
| **Mn** | bdl | bdl | bdl | bdl | bdl | 0.03 | 0.04 | 0.02 | bdl | 0.03 | bdl |
| **Sb** | 1.72 | 1.55 | 1.63 | 2.06 | 0.66 | 0.87 | 0.65 | 0.67 | 0.62 | 0.67 | 0.53 |
| **Bi** | bdl | 0.05 | bdl | bdl | 0.00 | 0.11 | 0.00 | bdl | bdl | bdl | bdl |
| **Cu** | bdl | bdl | bdl | bdl | bdl | bdl | bdl | bdl | bdl | bdl | bdl |
| **Ag** | 0.04 | bdl | bdl | bdl | bdl | 0.05 | 1.51 | 1.52 | 0.13 | 1.54 | 0.12 |
| **Zn** | bdl | 0.04 | 0.02 | 0.06 | bdl | bdl | 0.03 | bdl | bdl | bdl | bdl |
| **Pb** | 70.0 | 70.7 | 69.8 | 69.8 | 49.8 | 46.5 | 46.3 | 46.3 | 50.5 | 46.3 | 50.3 |
| **Fe** | bdl | bdl | 0.04 | 0.04 | bdl | bdl | 0.03 | 0.02 | 0.02 | 0.02 | bdl |
| **Total** | 97.7 | 98.5 | 97.8 | 98.0 | 96.7 | 98.0 | 96.8 | 97.9 | 97.1 | 97.5 | 97.3 |
| **[apfu]** | | | | | | | | | | | |
| **As** | 4.97 | 5.12 | 4.99 | 4.80 | 1.72 | 1.80 | 1.79 | 1.76 | 1.70 | 1.75 | 1.68 |
| **S** | 23 | 23 | 23 | 23 | 4 | 4 | 4 | 4 | 4 | 4 | 4 |
| **Tl** | 0.03 | 0.03 | 0.03 | 0.03 | 0.01 | 0.02 | 0.01 | 0.01 | 0.01 | 0.01 | 0.01 |
| **Mn** | | | | | | 0.00 | 0.00 | 0.00 | | 0.00 | |
| **Sb** | 0.61 | 0.55 | 0.57 | 0.72 | 0.03 | 0.04 | 0.03 | 0.03 | 0.03 | 0.03 | 0.02 |
| **Bi** | | 0.01 | | | 0.00 | 0.00 | 0.00 | | | | |
| **Cu** | | | | | | | | | | | |
| **Ag** | 0.02 | | | | | 0.00 | 0.08 | 0.07 | 0.01 | 0.08 | 0.01 |
| **Zn** | | 0.03 | 0.01 | 0.04 | | | 0.00 | | | | |
| **Pb** | 14.53 | 14.70 | 14.36 | 14.26 | 1.34 | 1.19 | 1.22 | 1.19 | 1.37 | 1.19 | 1.34 |
| **Fe** | | | 0.03 | 0.03 | | | 0.00 | 0.00 | 0.00 | 0.00 | |
| **(As+Sb)/S** | 0.24 | 0.25 | 0.24 | 0.24 | 0.44 | 0.46 | 0.45 | 0.45 | 0.43 | 0.45 | 0.43 |
| **As/Sb** | 8 | 9 | 9 | 7 | 56 | 48 | 61 | 60 | 59 | 60 | 70 |
| **Tl/As** | 0.005 | 0.005 | 0.006 | 0.006 | 0.004 | 0.008 | 0.006 | 0.005 | 0.005 | 0.005 | 0.005 |
| **Pb/Tl** | 544 | 581 | 453 | 518 | 182 | 78 | 120 | 123 | 165 | 149 | 175 |

**Tab. 2 Major element composition of various sulfosalts (continued)**

| Sample | Bin13 | Bin13 | Bin13 | Bin13 | Bin13 | Bin13 | Bin13 | Bin13 | Bin8 | Bin8 | Bin8 |
|---|---|---|---|---|---|---|---|---|---|---|---|
| Locality | Lengenbach | Lengenbach | Lengenbach | Lengenbach | Lengenbach | Lengenbach | Lengenbach | Lengenbach | Pizzo Cervandone | Pizzo Cervandone | Pizzo Cervandone |
| Mineral | Sulfide melt | Sulfide melt | Sulfide melt | Sulfide melt | Sulfide melt | Sulfide melt | Sulfide melt | Sulfide melt | Fahlore | Fahlore | Fahlore |
| [wt%] | | | | | | | | | | | |
| As | 27.1 | 27.1 | 27.2 | 28.0 | 33.3 | 27.3 | 27.7 | 27.1 | 19.3 | 19.4 | 19.6 |
| S | 25.9 | 26.2 | 26.3 | 26.4 | 27.9 | 26.1 | 26.3 | 26.0 | 28.2 | 28.3 | 28.6 |
| Tl | 5.46 | 5.04 | 6.74 | 10.3 | 18.0 | 5.49 | 6.76 | 6.19 | bdl | bdl | bdl |
| Mn | 0.03 | 0.03 | 0.02 | 0.03 | 0.02 | 0.02 | bdl | 0.03 | bdl | bdl | bdl |
| Sb | 0.51 | 0.60 | 0.86 | 1.01 | 0.32 | 0.60 | 0.77 | 0.57 | 0.32 | 0.29 | 0.34 |
| Bi | bdl | bdl | bdl | bdl | bdl | bdl | bdl | bdl | 1.19 | 1.38 | 1.14 |
| Cu | 0.15 | 0.10 | bdl | 0.01 | 0.22 | 0.13 | 0.04 | 0.03 | 43.2 | 43.1 | 43.4 |
| Ag | bdl | bdl | 0.06 | bdl | bdl | bdl | 0.03 | bdl | 0.19 | 0.24 | 0.20 |
| Zn | bdl | bdl | bdl | bdl | bdl | bdl | bdl | bdl | 3.42 | 3.37 | 3.44 |
| Pb | 40.9 | 41.3 | 38.6 | 34.2 | 19.2 | 40.1 | 38.3 | 39.3 | bdl | bdl | bdl |
| Fe | 0.03 | bdl | 0.00 | bdl | bdl | bdl | bdl | bdl | 4.30 | 4.34 | 4.33 |
| Total | 100.1 | 100.5 | 99.7 | 100.0 | 99.0 | 99.7 | 99.9 | 99.3 | 100.1 | 100.5 | 101.0 |
| | | | | | | | | | | | |
| [apfu] | | | | | | | | | | | |
| As | 0.45 | 0.44 | 0.44 | 0.45 | 0.51 | 0.45 | 0.45 | 0.45 | 3.81 | 3.81 | 3.81 |
| S | 1 | 1 | 1 | 1 | 1 | 1 | 1 | 1 | 13 | 13 | 13 |
| Tl | 0.03 | 0.03 | 0.04 | 0.06 | 0.10 | 0.03 | 0.04 | 0.04 | | | |
| Mn | 0.00 | 0.00 | 0.00 | 0.00 | 0.00 | 0.00 | | 0.00 | | | |
| Sb | 0.01 | 0.01 | 0.01 | 0.01 | 0.00 | 0.01 | 0.01 | 0.01 | 0.04 | 0.04 | 0.04 |
| Bi | | | | | | | | | 0.08 | 0.10 | 0.08 |
| Cu | 0.00 | 0.00 | 0.00 | 0.00 | 0.00 | 0.00 | 0.00 | 0.00 | 11.92 | 11.84 | 11.83 |
| Ag | | | 0.00 | | | | 0.00 | | 0.03 | 0.03 | 0.03 |
| Zn | | | 0.00 | | | | | | 0.77 | 0.76 | 0.77 |
| Pb | 0.24 | 0.24 | 0.23 | 0.20 | 0.11 | 0.24 | 0.23 | 0.23 | | | |
| Fe | 0.00 | | 0.00 | 0.00 | | | | | 1.14 | 1.14 | 1.13 |
| | | | | | | | | | | | |
| (As+Sb)/S | 0.45 | 0.45 | 0.45 | 0.46 | 0.51 | 0.45 | 0.46 | 0.45 | 0.30 | 0.30 | 0.30 |
| As/Sb | 86 | 74 | 52 | 45 | 169 | 74 | 58 | 77 | 98 | 107 | 93 |
| Tl/As | 0.07 | 0.07 | 0.09 | 0.13 | 0.20 | 0.07 | 0.09 | 0.08 | | | |
| Pb/Tl | 7.39 | 8.10 | 5.64 | 3.27 | 1.05 | 7.20 | 5.59 | 6.27 | | | |

**Tab. 2 Major element composition of various sulfosalts (continued)**

| **Sample** | Bin7 | Bin7 | Bin7 | Bin7 | Bin7 |
|---|---|---|---|---|---|
| **Locality** | Pizzo Cervandone | Pizzo Cervandone | Pizzo Cervandone | Pizzo Cervandone | Pizzo Cervandone |
| **Mineral** | Fahlore | Fahlore | Fahlore | Fahlore | Fahlore |
| **[wt% ]** | | | | | |
| **As** | 19.2 | 19.3 | 19.2 | 19.2 | 19.1 |
| **S** | 27.5 | 27.8 | 27.7 | 28.0 | 27.2 |
| **Tl** | bdl | bdl | bdl | bdl | bdl |
| **Mn** | bdl | bdl | bdl | bdl | bdl |
| **Sb** | 0.32 | 0.33 | 0.30 | 0.33 | 0.32 |
| **Bi** | 1.20 | 1.07 | 1.31 | 1.10 | 1.11 |
| **Cu** | 43.6 | 43.7 | 43.2 | 43.4 | 43.2 |
| **Ag** | 0.23 | 0.24 | 0.28 | 0.18 | 0.24 |
| **Zn** | 3.54 | 3.88 | 3.80 | 3.70 | 3.72 |
| **Pb** | bdl | bdl | bdl | bdl | bdl |
| **Fe** | 4.11 | 4.03 | 3.90 | 4.13 | 3.89 |
| **Total** | 99.6 | 100.3 | 99.7 | 100.1 | 98.9 |
| | | | | | |
| **[apfu]** | | | | | |
| **As** | 3.88 | 3.88 | 3.86 | 3.82 | 3.92 |
| **S** | 13 | 13 | 13 | 13 | 13 |
| **Tl** | | | | | |
| **Mn** | | | | | |
| **Sb** | 0.04 | 0.04 | 0.04 | 0.04 | 0.04 |
| **Bi** | 0.09 | 0.08 | 0.09 | 0.08 | 0.08 |
| **Cu** | 12.33 | 12.24 | 12.15 | 12.06 | 12.37 |
| **Ag** | 0.03 | 0.03 | 0.04 | 0.03 | 0.03 |
| **Zn** | 0.82 | 0.89 | 0.87 | 0.84 | 0.87 |
| **Pb** | | | | | |
| **Fe** | 1.12 | 1.08 | 1.05 | 1.10 | 1.07 |
| | | | | | |
| **(As+Sb)/S** | 0.30 | 0.30 | 0.30 | 0.30 | 0.30 |
| **As/Sb** | 97 | 96 | 104 | 94 | 98 |
| **Tl/As** | | | | | |
| **Pb/Tl** | | | | | |

**Tab. 3 Major and trace element composition of fissure micas, determined by EMPA and LA-ICP-MS, respectively.**

| **Mineral** | Muscovite | Muscovite | Muscovite | Muscovite | | | | | |
|---|---|---|---|---|---|---|---|---|---|
| **Locality** | Lengenbach | Balmen | Lengenbach | Gischi | | | | | |
| **Host rock** | Lengenbacher stratum | | Lengenbacher stratum | orthogneiss | | | | | |
| **Sample** | Bin 18 | Bin23 | Bin16 | Bin22 | | | | | |
| **[wt%]** | | | | | | | | | |
| F | 0.41 | 2.80 | 0.58 | 0.64 | | | | | |
| Na2O | 0.33 | 0.24 | 0.35 | 0.22 | | | | | |
| K2O | 10.7 | 9.0 | 10.2 | 10.8 | | | | | |
| Cl | 0.01 | 0.03 | 0.02 | 0.01 | | | | | |
| MgO | 2.53 | 26.6 | 3.88 | 2.59 | | | | | |
| CaO | b.d.l. | b.d.l. | 0.13 | b.d.l. | | | | | |
| BaO | 1.33 | 1.71 | 0.42 | 0.04 | | | | | |
| Al2O3 | 32.7 | 14.1 | 28.3 | 28.7 | | | | | |
| MnO | b.d.l. | b.d.l. | 0.04 | 0.11 | | | | | |
| TiO2 | 0.83 | 0.18 | 0.75 | 0.28 | | | | | |
| SiO2 | 48.1 | 43.7 | 49.2 | 48.1 | | | | | |
| FeO | b.d.l. | 0.13 | 0.11 | 4.33 | | | | | |
| Cr2O3 | 0.05 | b.d.l. | 1.37 | b.d.l. | | | | | |
| Total | 97.0 | 98.5 | 95.3 | 95.9 | | | | | |
| -F,Cl=O | 0.17 | 1.18 | 0.25 | 0.27 | | | | | |
| H2O | 3.96 | 2.63 | 3.82 | 3.74 | | | | | |
| **Total** | **100.7** | **99.9** | **98.9** | **99.3** | | | | | |
| **[µg/g]** | | | | | | | | | |
| Li | 418 | 427 | 404 | 548 | 240 | 224 | 763 | 762 | 1806 |
| As | b.d.l. | b.d.l. | b.d.l. | b.d.l. | b.d.l. | b.d.l. | b.d.l. | b.d.l. | 9.94 |
| Rb | 375 | 367 | 368 | 361 | 269 | 267 | 1554 | 1577 | 2534 |
| Sr | 7.71 | 15.9 | 8.59 | 37.8 | 428 | 284 | 3.83 | 3.92 | 2.76 |
| Y | b.d.l. | 0.177 | 0.135 | 0.337 | 5.46 | 2.03 | 2.28 | b.d.l. | 6.58 |
| Zr | b.d.l. | 0.176 | 0.151 | b.d.l. | 0.330 | 1.12 | 0.390 | 0.406 | b.d.l. |
| Nb | 1.00 | 1.54 | 2.38 | 2.31 | 7.70 | 5.32 | 95.6 | 98.5 | 96.5 |
| Sn | 28.8 | 34.7 | 45.6 | 4.23 | 6.75 | 8.68 | 392 | 408 | 108 |
| Sb | b.d.l. | b.d.l. | b.d.l. | b.d.l. | b.d.l. | b.d.l. | b.d.l. | b.d.l. | 0.730 |
| Cs | 8.48 | 9.03 | 8.66 | 37.8 | 6.33 | 6.91 | 84.0 | 85.2 | 523 |
| La | 0.026 | b.d.l. | b.d.l. | 0.670 | 17.4 | 6.79 | 0.434 | b.d.l. | 0.554 |
| Ce | b.d.l. | 0.126 | 0.021 | 0.950 | 19.4 | 8.08 | 1.08 | b.d.l. | 2.03 |
| Pr | b.d.l. | b.d.l. | b.d.l. | 0.141 | 1.74 | 0.930 | 0.179 | b.d.l. | 0.213 |
| Nd | b.d.l. | b.d.l. | b.d.l. | b.d.l. | 7.34 | 2.44 | 0.730 | b.d.l. | 1.09 |
| Sm | b.d.l. | b.d.l. | b.d.l. | b.d.l. | 1.29 | b.d.l. | b.d.l. | b.d.l. | 0.260 |
| Eu | 0.369 | 0.308 | 0.390 | 0.383 | 0.352 | b.d.l. | b.d.l. | b.d.l. | 0.078 |
| Gd | b.d.l. | b.d.l. | b.d.l. | b.d.l. | b.d.l. | b.d.l. | b.d.l. | b.d.l. | 0.720 |
| Tb | b.d.l. | b.d.l. | b.d.l. | b.d.l. | b.d.l. | 0.103 | 0.064 | b.d.l. | 0.132 |
| Dy | b.d.l. | b.d.l. | b.d.l. | b.d.l. | b.d.l. | b.d.l. | b.d.l. | b.d.l. | 1.31 |
| Ho | b.d.l. | b.d.l. | b.d.l. | b.d.l. | b.d.l. | b.d.l. | 0.133 | b.d.l. | 0.940 |
| Er | b.d.l. | b.d.l. | b.d.l. | b.d.l. | b.d.l. | b.d.l. | 0.267 | b.d.l. | 0.470 |
| Tm | b.d.l. | b.d.l. | b.d.l. | b.d.l. | b.d.l. | b.d.l. | 0.054 | b.d.l. | 0.098 |
| Yb | b.d.l. | b.d.l. | b.d.l. | b.d.l. | 0.460 | 0.210 | 0.630 | 0.390 | 23.7 |
| Lu | b.d.l. | b.d.l. | b.d.l. | b.d.l. | b.d.l. | b.d.l. | 0.179 | 0.189 | 0.070 |
| Hf | 0.219 | 0.050 | b.d.l. | b.d.l. | b.d.l. | b.d.l. | b.d.l. | b.d.l. | b.d.l. |
| Ta | 0.487 | 0.285 | 0.449 | 0.090 | 0.193 | 0.102 | 22.7 | 22.2 | 40.3 |
| Tl | 346 | 334 | 330 | 8.11 | 50.7 | 47.2 | 6.07 | 6.03 | 20.4 |
| Pb | 3.52 | 1.19 | 2.88 | 49.9 | 21.2 | 42.1 | 7.52 | 8.59 | 171 |
| Th | b.d.l. | b.d.l. | b.d.l. | 2.56 | 0.380 | 0.227 | 0.108 | 0.050 | 1.09 |
| U | b.d.l. | 0.027 | 0.014 | 0.098 | 0.950 | 0.187 | 0.181 | b.d.l. | 3.31 |
| K/Rb | 237 | 243 | 242 | 207 | 313 | 316 | 57.8 | 57.0 | 35.5 |
| K/Tl | 258 | 267 | 270 | 9234 | 1661 | 1786 | 14799 | 14897 | 4408 |
| Rb/Tl | 1.09 | 1.10 | 1.11 | 44.5 | 5.31 | 5.66 | 256 | 262 | 124 |

**Tab. 3 Major and trace element composition of fissure micas (continued)**

| Muscovite<br>Pizzo<br>orthogneiss<br>Bin20 | Muscovite<br>Messerbach<br>Lengenbacher stratum<br>Bin21 | Muscovite<br>Gorb<br>orthogneiss<br>B5108 |
|---|---|---|
| 3.41 | 0.20 | b.d.l. |
| 0.08 | 0.31 | 0.26 |
| 9.47 | 11.0 | 10.9 |
| b.d.l. | 0.01 | b.d.l. |
| 15.6 | 3.02 | 1.71 |
| b.d.l. | 0.03 | b.d.l. |
| b.d.l. | 0.21 | 0.12 |
| 14.9 | 31.3 | 30.0 |
| 0.42 | b.d.l. | 0.04 |
| 0.80 | 1.04 | 0.96 |
| 41.1 | 47.7 | 45.6 |
| 13.4 | 0.29 | 5.60 |
| 0.03 | 0.03 | b.d.l. |
| 99.1 | 95.1 | 95.1 |
| 1.44 | 0.08 | 0.00 |
| 2.14 | 4.01 | 4.00 |
| **99.8** | **99.1** | **99.1** |

| | | | | | | | | | |
|---|---|---|---|---|---|---|---|---|---|
| 791 | 943 | 769 | 899 | 268 | 260 | 264 | 263 | 520 | 512 |
| 28.8 | 74.9 | 20.9 | 56.7 | b.d.l. | b.d.l. | b.d.l. | b.d.l. | b.d.l. | 12.2 |
| 1513 | 1330 | 1487 | 1272 | 293 | 259 | 310 | 261 | 766 | 782 |
| 1.48 | 1.54 | 0.842 | 2.25 | 8.59 | 12.6 | 10.4 | 11.2 | 1.48 | 1.03 |
| 0.808 | 20.2 | 0.362 | 4.06 | 0.059 | 0.074 | b.d.l. | b.d.l. | b.d.l. | 0.130 |
| b.d.l. | 0.231 | b.d.l. | b.d.l. | 0.259 | 0.387 | 0.326 | 0.580 | 0.164 | b.d.l. |
| 21.0 | 40.7 | 20.8 | 22.4 | 8.26 | 11.6 | 5.02 | 21.1 | 44.4 | 42.1 |
| 94.8 | 102 | 94.9 | 85.0 | 10.4 | 13.3 | 8.46 | 18.4 | 7.80 | 7.68 |
| 0.670 | 1.41 | 0.500 | 1.98 | b.d.l. | b.d.l. | b.d.l. | 2.01 | 2.57 | 1.87 |
| 318 | 344 | 237 | 264 | 12.4 | 11.0 | 13.7 | 12.0 | 52.5 | 53.0 |
| b.d.l. | b.d.l. | b.d.l. | b.d.l. | b.d.l. | b.d.l. | b.d.l. | b.d.l. | b.d.l. | 0.057 |
| b.d.l. | 0.195 | 0.017 | 0.161 | 0.279 | b.d.l. | 0.120 | 0.065 | b.d.l. | b.d.l. |
| 0.017 | 0.068 | b.d.l. | 0.024 | b.d.l. | b.d.l. | 0.021 | b.d.l. | b.d.l. | b.d.l. |
| b.d.l. | 0.350 | b.d.l. | 0.333 | 0.187 | 0.099 | b.d.l. | b.d.l. | b.d.l. | 0.159 |
| 0.056 | b.d.l. | b.d.l. | 0.237 | b.d.l. | b.d.l. | b.d.l. | b.d.l. | b.d.l. | b.d.l. |
| b.d.l. | 0.116 | b.d.l. | b.d.l. | b.d.l. | b.d.l. | b.d.l. | b.d.l. | b.d.l. | b.d.l. |
| b.d.l. | 1.01 | b.d.l. | b.d.l. | b.d.l. | b.d.l. | b.d.l. | b.d.l. | b.d.l. | b.d.l. |
| b.d.l. | 0.311 | b.d.l. | 0.076 | b.d.l. | b.d.l. | b.d.l. | b.d.l. | b.d.l. | 0.021 |
| b.d.l. | 3.24 | b.d.l. | 0.520 | b.d.l. | b.d.l. | b.d.l. | b.d.l. | b.d.l. | b.d.l. |
| b.d.l. | 0.771 | b.d.l. | 0.141 | b.d.l. | b.d.l. | b.d.l. | b.d.l. | b.d.l. | b.d.l. |
| 0.043 | 3.03 | b.d.l. | 0.373 | b.d.l. | b.d.l. | b.d.l. | b.d.l. | b.d.l. | b.d.l. |
| b.d.l. | 0.519 | b.d.l. | 0.097 | b.d.l. | b.d.l. | b.d.l. | b.d.l. | b.d.l. | b.d.l. |
| 0.151 | 5.16 | b.d.l. | 0.610 | b.d.l. | b.d.l. | b.d.l. | b.d.l. | b.d.l. | b.d.l. |
| 0.018 | 0.606 | 0.018 | 0.133 | b.d.l. | b.d.l. | b.d.l. | b.d.l. | b.d.l. | 0.014 |
| b.d.l. | b.d.l. | 0.038 | b.d.l. | 0.115 | b.d.l. | b.d.l. | b.d.l. | 0.047 | b.d.l. |
| 0.287 | 2.18 | 0.233 | 0.413 | 0.272 | 0.401 | 0.164 | 0.847 | 3.84 | 4.09 |
| 14.6 | 15.4 | 14.2 | 14.0 | 2.28 | 1.91 | 2.29 | 1.93 | 6.99 | 6.52 |
| 30.0 | 44.1 | 17.6 | 102 | 5.20 | 5.82 | 14.0 | 9.01 | 3.94 | 5.60 |
| b.d.l. | b.d.l. | b.d.l. | b.d.l. | 0.344 | 0.205 | 0.493 | 0.560 | b.d.l. | 0.271 |
| 0.528 | 0.872 | 0.126 | 1.24 | b.d.l. | b.d.l. | b.d.l. | b.d.l. | 28.4 | 0.063 |
| 51.9 | 59.1 | 52.9 | 61.8 | 311 | 350 | 294 | 348 | 118 | 116 |
| 5381 | 5095 | 5533 | 55997 | 39871 | 47645 | 39697 | 47102 | 12922 | 13854 |
| 104 | 86.2 | 105 | 90.6 | 128 | 136 | 135 | 135 | 110 | 120 |

**Tab. 3 Major and trace element composition of fissure micas (continued)**

| Muscovite<br>Gorb<br>orthogneiss<br>Bin26 | | | Biotite<br>Feldbach<br>Feldbacher stratum<br>Bin24 | | | | Muscovite<br>Turtschi<br>Feldbacher stratum<br>Bin30 | | |
|---|---|---|---|---|---|---|---|---|---|
| | | | | | | | | | |
| 0.12 | | | 1.15 | | | | 0.07 | | |
| 0.63 | | | 0.07 | | | | 0.52 | | |
| 10.2 | | | 9.32 | | | | 10.5 | | |
| b.d.l. | | | 0.01 | | | | b.d.l. | | |
| 3.00 | | | 19.9 | | | | 2.98 | | |
| b.d.l. | | | b.d.l. | | | | b.d.l. | | |
| 0.36 | | | 0.05 | | | | 0.28 | | |
| 32.0 | | | 13.6 | | | | 31.6 | | |
| b.d.l. | | | b.d.l. | | | | b.d.l. | | |
| 0.68 | | | 0.30 | | | | 0.53 | | |
| 48.6 | | | 41.2 | | | | 49.0 | | |
| 0.47 | | | 11.6 | | | | 0.43 | | |
| b.d.l. | | | b.d.l. | | | | b.d.l. | | |
| 96.1 | | | 97.1 | | | | 96.0 | | |
| 0.05 | | | 0.49 | | | | 0.03 | | |
| 4.11 | | | 3.25 | | | | 4.13 | | |
| **100.1** | | | **99.9** | | | | **100.1** | | |
| | | | | | | | | | |
| 473 | 492 | 459 | 435 | 416 | 425 | 436 | 193 | 167 | 153 |
| 40.2 | 79.6 | 19.7 | b.d.l. | b.d.l. | b.d.l. | b.d.l. | b.d.l. | b.d.l. | b.d.l. |
| 792 | 726 | 921 | 409 | 408 | 408 | 414 | 432 | 413 | 349 |
| 7.43 | 15.8 | 2.13 | 0.422 | 0.381 | 0.233 | 0.540 | 0.760 | 3.78 | 13.5 |
| 17.6 | 40.5 | 1.39 | 0.053 | b.d.l. | b.d.l. | b.d.l. | b.d.l. | 0.280 | 1.49 |
| 0.064 | b.d.l. | b.d.l. | 0.028 | b.d.l. | 0.034 | b.d.l. | b.d.l. | 0.224 | 0.278 |
| 53.3 | 47.2 | 50.2 | 24.1 | 24.6 | 24.7 | 24.7 | 28.8 | 27.6 | 34.5 |
| 7.43 | 6.16 | 6.34 | 4.65 | 4.52 | 4.31 | 5.11 | 8.60 | 8.52 | 13.0 |
| 3.95 | 4.15 | 4.23 | 0.650 | 0.750 | 0.820 | 0.940 | b.d.l. | b.d.l. | b.d.l. |
| 60.2 | 73.7 | 59.5 | 142 | 139 | 124 | 129 | 9.66 | 9.77 | 6.37 |
| 68.1 | 116 | 4.10 | b.d.l. | b.d.l. | b.d.l. | b.d.l. | b.d.l. | b.d.l. | 0.148 |
| 23.7 | 59.3 | 2.94 | 0.011 | b.d.l. | 0.013 | b.d.l. | b.d.l. | 0.045 | 0.428 |
| 12.5 | 23.5 | 0.813 | b.d.l. | b.d.l. | b.d.l. | b.d.l. | 0.012 | b.d.l. | 0.075 |
| 47.2 | 87.8 | 2.77 | b.d.l. | b.d.l. | b.d.l. | b.d.l. | b.d.l. | 0.206 | 0.420 |
| 5.73 | 12.6 | 0.400 | b.d.l. | b.d.l. | b.d.l. | b.d.l. | b.d.l. | b.d.l. | b.d.l. |
| 0.639 | 1.55 | 0.110 | b.d.l. | b.d.l. | 0.020 | 0.034 | b.d.l. | b.d.l. | b.d.l. |
| 4.17 | 7.16 | 0.316 | b.d.l. | b.d.l. | b.d.l. | b.d.l. | b.d.l. | b.d.l. | b.d.l. |
| 0.271 | 0.601 | b.d.l. | b.d.l. | b.d.l. | b.d.l. | b.d.l. | b.d.l. | 0.018 | b.d.l. |
| 1.53 | 3.38 | b.d.l. | b.d.l. | b.d.l. | b.d.l. | b.d.l. | b.d.l. | 0.130 | 0.364 |
| 0.269 | 0.964 | 0.036 | b.d.l. | b.d.l. | b.d.l. | b.d.l. | b.d.l. | b.d.l. | 0.036 |
| 1.20 | 3.53 | b.d.l. | b.d.l. | b.d.l. | b.d.l. | b.d.l. | b.d.l. | b.d.l. | b.d.l. |
| 0.196 | 0.659 | b.d.l. | b.d.l. | b.d.l. | b.d.l. | b.d.l. | b.d.l. | b.d.l. | b.d.l. |
| 2.02 | 6.23 | b.d.l. | b.d.l. | b.d.l. | b.d.l. | b.d.l. | b.d.l. | b.d.l. | b.d.l. |
| 0.394 | 1.12 | 0.040 | b.d.l. | b.d.l. | b.d.l. | b.d.l. | b.d.l. | b.d.l. | b.d.l. |
| b.d.l. | b.d.l. | b.d.l. | b.d.l. | b.d.l. | b.d.l. | 0.074 | b.d.l. | b.d.l. | b.d.l. |
| 3.08 | 3.19 | 3.51 | 1.17 | 1.21 | 1.27 | 1.26 | 3.02 | 2.75 | 3.60 |
| 7.33 | 7.92 | 8.07 | 6.20 | 5.97 | 5.78 | 7.34 | 2.81 | 2.70 | 2.51 |
| 27.5 | 42.2 | 16.4 | 6.82 | 4.89 | 6.66 | 11.0 | 0.269 | 1.22 | 2.96 |
| 0.142 | 0.397 | b.d.l. | 1.51 | 1.31 | 1.65 | 1.14 | b.d.l. | 0.079 | 0.070 |
| 1.69 | 0.558 | 0.023 | 0.088 | 0.062 | 0.086 | 0.444 | b.d.l. | 0.110 | b.d.l. |
| | | | | | | | | | |
| 107 | 117 | 92.2 | 189 | 190 | 190 | 187 | 202 | 212 | 251 |
| 11575 | 10713 | 10514 | 12480 | 12961 | 13387 | 10542 | 31110 | 32378 | 34829 |
| 108 | 91.7 | 114 | 66.0 | 68.3 | 70.5 | 56.4 | 154 | 153 | 139 |

**Tab. 3 Major and trace element composition of fissure micas (continued)**

| Muscovite Schinhorn orthogneiss Bin28 | Muscovite Ritterpass orthogneiss Bin25 |
|---|---|
| 0.04 | 1.54 |
| 0.21 | 0.06 |
| 10.9 | 9.45 |
| b.d.l. | b.d.l. |
| 1.44 | 15.7 |
| b.d.l. | b.d.l. |
| 0.10 | b.d.l. |
| 30.5 | 16.0 |
| b.d.l. | 0.65 |
| 0.80 | 1.45 |
| 46.0 | 40.9 |
| 5.50 | 12.5 |
| b.d.l. | b.d.l. |
| 95.6 | 98.3 |
| 0.02 | 0.65 |
| 4.00 | 3.09 |
| **99.6** | **100.7** |
| | |
| 88.1 | 81.1 | 78.1 | 73.8 | 797 | 836 | 887 |
| b.d.l. | b.d.l. | b.d.l. | b.d.l. | b.d.l. | b.d.l. | b.d.l. |
| 447 | 479 | 524 | 503 | 971 | 997 | 1006 |
| 11.5 | 12.7 | 6.68 | 7.14 | 1.06 | 0.939 | 0.343 |
| b.d.l. | b.d.l. | b.d.l. | b.d.l. | 2.74 | 5.44 | 0.350 |
| 0.058 | 0.186 | 0.394 | 0.226 | 0.295 | 0.226 | 0.186 |
| 15.6 | 31.6 | 30.10 | 63.0 | 250 | 263 | 182 |
| 4.62 | 7.65 | 8.40 | 23.2 | 22.9 | 23.6 | 20.4 |
| b.d.l. | b.d.l. | b.d.l. | b.d.l. | b.d.l. | 0.780 | 0.600 |
| 7.35 | 8.55 | 8.77 | 6.82 | 123 | 121 | 130 |
| b.d.l. | b.d.l. | b.d.l. | b.d.l. | 13.4 | 29.8 | 1.08 |
| b.d.l. | b.d.l. | 0.031 | b.d.l. | 17.6 | 14.0 | 2.81 |
| b.d.l. | b.d.l. | b.d.l. | b.d.l. | 2.81 | 6.24 | 0.272 |
| 0.078 | b.d.l. | b.d.l. | b.d.l. | 10.7 | 22.7 | 0.970 |
| b.d.l. | b.d.l. | b.d.l. | b.d.l. | 1.68 | 3.34 | 0.183 |
| 0.082 | b.d.l. | 0.054 | 0.033 | 0.101 | 0.226 | 0.013 |
| b.d.l. | b.d.l. | b.d.l. | b.d.l. | 0.980 | 3.14 | b.d.l. |
| b.d.l. | b.d.l. | b.d.l. | b.d.l. | 0.175 | 0.262 | b.d.l. |
| b.d.l. | b.d.l. | b.d.l. | b.d.l. | 0.540 | 1.22 | b.d.l. |
| b.d.l. | b.d.l. | b.d.l. | b.d.l. | 0.079 | 0.172 | b.d.l. |
| b.d.l. | b.d.l. | b.d.l. | b.d.l. | 0.212 | 0.385 | b.d.l. |
| b.d.l. | b.d.l. | b.d.l. | b.d.l. | b.d.l. | b.d.l. | 0.007 |
| b.d.l. | b.d.l. | 0.067 | b.d.l. | 0.111 | 0.318 | b.d.l. |
| b.d.l. | b.d.l. | b.d.l. | b.d.l. | 0.034 | 0.056 | b.d.l. |
| b.d.l. | b.d.l. | 0.098 | 0.056 | b.d.l. | b.d.l. | 0.026 |
| 0.728 | 1.46 | 0.452 | 2.12 | 13.5 | 14.0 | 10.6 |
| 2.51 | 2.57 | 2.31 | 2.10 | 5.59 | 5.44 | 5.71 |
| 6.04 | 9.11 | 3.73 | 3.79 | 4.22 | 3.73 | 1.50 |
| b.d.l. | b.d.l. | 0.061 | b.d.l. | 0.063 | 0.108 | 0.012 |
| b.d.l. | 0.017 | b.d.l. | b.d.l. | 1.13 | 1.19 | 0.225 |
| | | | | | | |
| 203 | 190 | 173 | 181 | 80.8 | 78.7 | 78.0 |
| 36185 | 35340 | 39250 | 43353 | 14035 | 14422 | 13740 |
| 178 | 186 | 227 | 240 | 174 | 183 | 176 |

**Table 4 Results of Tl isotope analysis**

| | | | $\varepsilon^{205}$Tl | ±2sd | n |
|---|---|---|---|---|---|
| **reference materials** | | | | | |
| Aldrich Tl | | this study | -0.8 | 0.6 | 3 |
| | | reference value | -0.81 | 0.33 | |
| AGV-2 | | this study | -3.6 | 0.6 | 3 |
| | | reference value | -3.0 | 0.6 | |
| | | | | | |
| **samples** | **locality** | **mineral** | $\varepsilon^{205}$Tl | ±2sd | n |
| Bin 1 | Lengenbach quarry | jordanite | -4.1 | 0.5 | 2 |
| Bin 2 | Lengenbach quarry | fahlore | 1.1 | 0.5 | 2 |
| Bin 3 | Lengenbach quarry | jordanite | -1.5 | 0.5 | 2 |
| Bin 4 | Lengenbach quarry | hatchite | 0.6 | 0.5 | 1 |
| Bin 5 | Lengenbach quarry | fahlore | 1.0 | 0.5 | 1 |
| Bin 6 | Lengenbach quarry | edenharterite | 1.9 | 0.5 | 2 |
| Bin 7 | Pizzo Cervandone | fahlore | 0.1 | 0.7 | 1 |
| Bin 8 | Pizzo Cervandone | fahlore | -3.0 | 0.6 | 1 |
| Bin 9 | Lengenbach quarry | sartorite | -2.2 | 0.5 | 2 |
| Bin 10 | Pizzo Cervandone | asbecasite | -2.0 | 0.5 | 1 |
| Bin 11 | Lengenbach quarry | orpiment | 1.1 | 0.5 | 1 |
| Bin 12 | Lengenbach quarry | sartorite | -0.5 | 0.5 | 2 |
| Bin 13 | Lengenbach quarry | melt inclusions | -0.3 | 0.5 | 2 |
| BG 186 | Wiesloch | galenite | -1.4 | 0.5 | 1 |
| BW114 | Wiesloch | sphalerite | -2.7 | 0.5 | 1 |

n = number of individual analyses conducted on the same sample solution
The reference values for Aldrich Tl and AGV-2 are from Nielsen and Rehkämper (2011)